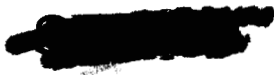


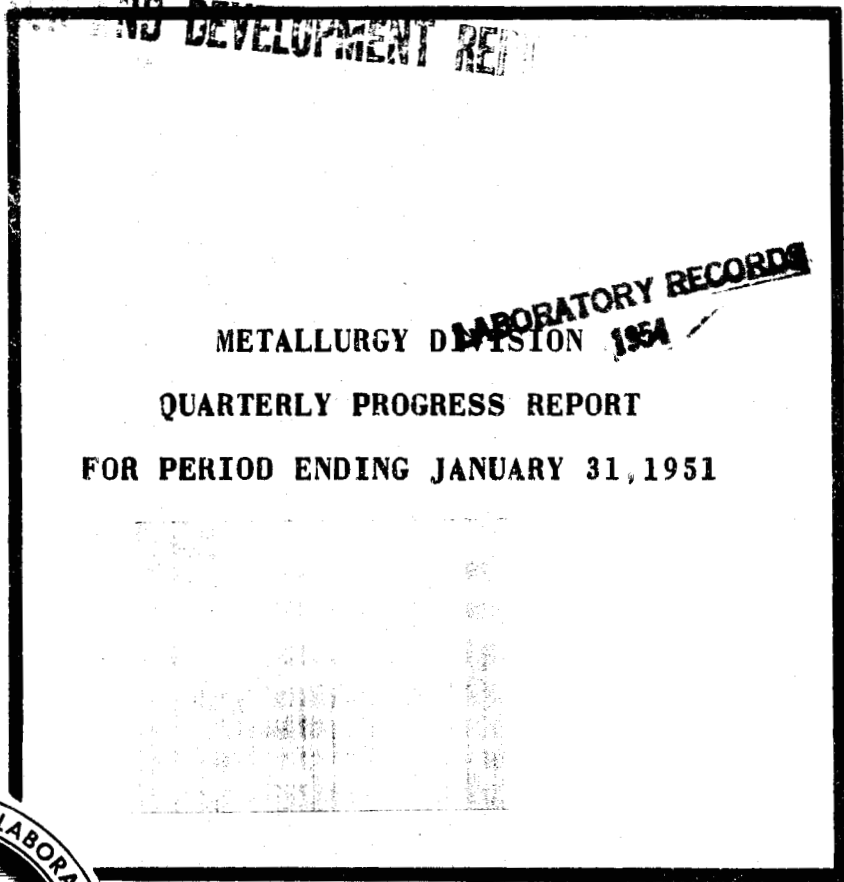


3 4456 0360860 1

ORNL 987
Progress Report
90



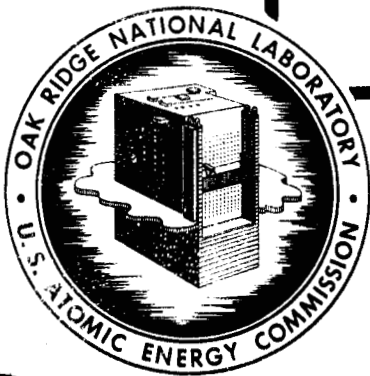
RESEARCH AND DEVELOPMENT REPORT



METALLURGY DIVISION **LABORATORY RECORDS**
1951

QUARTERLY PROGRESS REPORT

FOR PERIOD ENDING JANUARY 31, 1951



DECLASSIFIED

CLASSIFICATION CHANGED BY

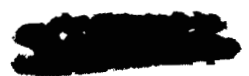
BY AUTHORITY OF: AEC-6-12-62
BY: N. Bluman 8.14.62



OAK RIDGE NATIONAL LABORATORY
OPERATED BY
CARBIDE AND CARBON CHEMICALS COMPANY
A DIVISION OF UNION CARBIDE AND CARBON CORPORATION



POST OFFICE BOX P
OAK RIDGE, TENNESSEE



~~SECRET~~

ORNL-987
Progress Report

This document consists of 76 pages.
Copy 9 of 128 . Series A.

Contract No. W-7405, eng 26

METALLURGY DIVISION

J. H. Frye, Jr., Director

**QUARTERLY PROGRESS REPORT
for Period Ending January 31, 1951**

Edited by

E. C. Miller and W. H. Bridges

Date Issued JUN 7 1951

~~RESTRICTED DATA~~
This document contains restricted data as defined in the Energy Handbook.

~~SECRET~~

its trans-
any use
and
app



ing the
ents in
hibited
es under

3 4456 0360860 1

OAK RIDGE NATIONAL LABORATORY
operated by
CARBIDE AND CARBON CHEMICALS COMPANY
A Division of Union Carbide and Carbon Corporation
Post Office Box P
Oak Ridge, Tennessee

~~SECRET~~

~~SECRET~~

INTERNAL DISTRIBUTION

- | | | |
|------------------------------|-----------------------|-----------------------------|
| 1. G. Felbeck (C&CCC) | 28. W. H. Pennington | 50. Anton Brasunas |
| 2-3. Chemistry Library | 29. F. L. Steahly | 51. R. Crouse |
| 4. Physics Library | 30. A. H. Snell | 52. B. E. Adams |
| 5. Biology Library | 31. R. C. Briant | 53. J. H. Erwin |
| 6. Health Physics Library | 32. C. P. Keim | 54. J. O. Betterton, Jr. |
| 7. Metallurgy Library | 33. G. H. Clewett | 55. R. O. Williams |
| 8-9. Training School Library | 34. W. H. Bridges | 56. G. M. Adamson |
| 10-13. Central Files | 35. A. G. H. Andersen | 57. E. S. Bomar |
| 14. C. E. Center | 36. L. K. Jetter | 58. L. A. Abrams |
| 15. C. E. Larson | 37. E. J. Boyle | 59. R. B. Day |
| 16. W. B. Humes (K-25) | 38. W. D. Manly | 60. T. W. Fulton |
| 17. W. D. Lavers (Y-12) | 39. C. D. Susano | 61. F. W. Drosten |
| 18. A. M. Weinberg | 40. W. W. Parkinson | 62. R. B. Oliver |
| 19. J. A. Swartout | 41. R. J. Gray | 63. P. Patriarca |
| 20. E. D. Shipley | 42. B. S. Borie | 64. J. T. Howe |
| 21. E. J. Murphy | 43. D. S. Billington | 65. T. H. Blewitt |
| 22. F. C. VonderLage | 44. C. D. Smith | 66. W. E. Taylor |
| 23. E. H. Taylor | 45. D. E. Harby | 67. J. H. Crawford, Jr. |
| 24. J. H. Frye | 46. E. E. Scansbury | 68. A. F. Cohen |
| 25. K. Z. Morgan | 47. G. P. Smith | 69. J. C. Wilson |
| 26. D. W. Cardwell | 48. F. Cunningham | 70. H. W. Savage |
| 27. M. T. Kelley | 49. E. C. Miller | 71-72. Central Files (O.P.) |

EXTERNAL DISTRIBUTION

- 73-80. Argonne National Laboratory
- 81-83. Atomic Energy Commission, Washington
- 84-87. Brookhaven National Laboratory
- 88-91. Carbide and Carbon Chemicals Company (Y-12)
- 92-93. Knolls Atomic Power Laboratory
- 94-95. General Electric Company, Richland
- 96. Hanford Directed Operations
- 97-100. Los Alamos
- 101-102. New York Operations Office
- 103. Patent Branch, Washington
- 104-118. Technical Information Branch, ORE
- 119-122. University of California Radiation Laboratory
- 123. Massachusetts Institute of Technology (Kaufmann)
- 124. Battelle Memorial University
- 125-127. NEPA
- 128. Savannah River Operations Office, Wilmington

~~SECRET~~

Other Oak Ridge National Laboratory reports in this series are as follows:

Period Ending March 1, 1948	ORNL 28
Period Ending May 31, 1948	ORNL 69
Period Ending July 31, 1949	ORNL 407
Period Ending October 31, 1949	ORNL 511
Period Ending January 31, 1950	ORNL 583
Period Ending April 30, 1950	ORNL 754
Period Ending July 31, 1950	ORNL 827
Period Ending October 31, 1950	ORNL 910

~~SECRET~~

~~SECRET~~

TABLE OF CONTENTS

SUMMARY	7
1. THORIUM RESEARCH	9
Thermal Cycling of Thorium	9
Metallography of Thorium	9
Fabrication of Thorium	10
Extrusion	10
Rolling and swaging	12
Drawing	12
Work Hardening of Iodide-process Thorium	12
Recrystallization of Thorium	13
Shear Modulus of Thorium	13
2. URANIUM RESEARCH	17
Fabrication of Uranium Tubing	17
Preferred Orientation and Anisotropy in Properties of Metals	17
Uranium Bonding Studies	36
3. ANP PROGRAM	38
Liquid-metal Corrosion Testing	38
Revision of static corrosion-testing technique	38
Static corrosion-test data	38
Dynamic corrosion testing	48
Powder Metallurgy — Fuel Element Fabrication	52
Sintering a loose powder	52
MTR type fuel plate	57
Compatibility test of potential fuel element materials	62
Creep-Rupture Laboratory	64
Welding Laboratory	65
Welding of refractory metals	66
Thermal convection loop fabrication	66
Seam-welding of flattened tube ends	66
Physical Chemistry of Liquid Metals	67
Hydrogenous fluids	67
Corrosion of metal single crystals by liquid metals	67
4. MTR FUEL ELEMENTS	71
5. SERVICE WORK	72
KAPL Disks	72
Boral Rolling	72
ANP Disks	72
6. LIST OF PERSONNEL	74

~~SECRET~~

LIST OF FIGURES

Fig. 1.1	Extruded Thorium	11
Fig. 1.2	Strain Hardening Curves for Ames and Iodide Thorium	14
Fig. 1.3	Isothermal Recrystallization Curves for Thorium	15
Fig. 2.1	α -Extruded Uranium Tubing	18
Fig. 2.2	Sketch Showing the Dimensions of the X-ray Diffraction Specimens and the Location in the Sample of α -Extruded Uranium from Which They Were Machined	19
Fig. 2.3	Preferred Orientation Plot — (110) — 1½-in.-Diameter α -Extruded Uranium Rod	21
Fig. 2.4	Preferred Orientation Plot — (110) — 9/10-in.-Diameter α -Extruded Uranium Rod	21
Fig. 2.5	Preferred Orientation Plot — (110) — 5/8-in.-Diameter α -Extruded Uranium Rod	21
Fig. 2.6	Preferred Orientation Plot — (021) — 1½-in.-Diameter α -Extruded Uranium Rod	22
Fig. 2.7	Preferred Orientation Plot — (021) — 9/10-in.-Diameter α -Extruded Uranium Rod	22
Fig. 2.8	Preferred Orientation Plot — (021) — 5/8-in.-Diameter α -Extruded Uranium Rod	22
Fig. 2.9	Preferred Orientation Plot — (002) — 1½-in.-Diameter α -Extruded Uranium Rod	23
Fig. 2.10	Preferred Orientation Plot — (002) — 9/10-in.-Diameter α -Extruded Uranium Rod	23
Fig. 2.11	Preferred Orientation Plot — (002) — 5/8-in.-Diameter α -Extruded Uranium Rod	23
Fig. 2.12	Preferred Orientation Plot — (111) — 1½-in.-Diameter α -Extruded Uranium Rod	24
Fig. 2.13	Preferred Orientation Plot — (111) — 9/10-in.-Diameter α -Extruded Uranium Rod	24
Fig. 2.14	Preferred Orientation Plot — (111) — 5/8-in.-Diameter α -Extruded Uranium Rod	24
Fig. 2.15	Preferred Orientation Plot — (112) — 1½-in.-Diameter α -Extruded Uranium Rod	25
Fig. 2.16	Preferred Orientation Plot — (112) — 9/10-in.-Diameter α -Extruded Uranium Rod	25

Fig. 2.17	Preferred Orientation Plot — (112) — 5/8-in.-Diameter α -Extruded Uranium Rod	25
Fig. 2.18	Preferred Orientation Plot — (131) — 1½-in.-Diameter α -Extruded Uranium Rod	26
Fig. 2.19	Preferred Orientation Plot — (131) — 9/10-in.-Diameter α -Extruded Uranium Rod	26
Fig. 2.20	Preferred Orientation Plot — (131) — 5/8-in.-Diameter α -Extruded Uranium Rod	26
Fig. 2.21	Preferred Orientation Plot — (040) — 1½-in.-Diameter α -Extruded Uranium Rod	27
Fig. 2.22	Preferred Orientation Plot — (040) — 9/10-in.-Diameter α -Extruded Uranium Rod	27
Fig. 2.23	Preferred Orientation Plot — (040) — 5/8-in.-Diameter α -Extruded Uranium Rod	27
Fig. 2.24	Preferred Orientation Plot — (200) — 1½-in.-Diameter α -Extruded Uranium Rod	28
Fig. 2.25	Preferred Orientation Plot — (200) — 9/10-in.-Diameter α -Extruded Uranium Rod	28
Fig. 2.26	Preferred Orientation Plot — (200) — 5/8-in.-Diameter α -Extruded Uranium Rod	28
Fig. 2.27	Preferred Orientation Plot — (041) — 1½-in.-Diameter α -Extruded Uranium Rod	29
Fig. 2.28	Preferred Orientation Plot — (041) — 9/10-in.-Diameter α -Extruded Uranium Rod	29
Fig. 2.29	Preferred Orientation Plot — (041) — 5/8-in.-Diameter α -Extruded Uranium Rod	29
Fig. 2.30	Photomicrograph Showing the Deformed Grain Structure in the Middle of the Length of a 1½-in.-Diameter α -Extruded Uranium Rod	31
Fig. 2.31	Photomicrograph Showing the Partially Recrystallized Grain Structure in the Middle of the Length of 9/10-in.-Diameter α -Extruded Uranium Rod	32
Fig. 2.32	Photomicrograph Showing the Completely Recrystallized Grain Structure Near the Front End of a 5/8-in.-Diameter α -Extruded Uranium Rod	33
Fig. 2.33	Photomicrograph Showing the Almost Completely Recrystallized Grain Structure in the Middle of the Length of a 5/8-in.- Diameter α -Extruded Uranium Rod	34

Fig. 2.34	Photomicrograph Showing the Partially Recrystallized Grain Structure Near the Back End of a 5/8-in.-Diameter α -Extruded Uranium Rod	35
Fig. 3.1	Mass Transfer from Nickel Capsule to Molybdenum Specimen in Liquid Bismuth	41
Fig. 3.2	Corrosion Specimens Exposed to Sodium	42
Fig. 3.3	Type 304 Low-carbon Stainless Steel Exposed to Lead	41
Fig. 3.4	Stainless Steel Exposed to Lead	43
Fig. 3.5	Corrosion Tube Specimens Exposed to Bismuth-Uranium Alloy	44
Fig. 3.6	Clad 316--UO ₂ (20%) Powder Compact -- As-sintered	54
Fig. 3.7	Clad 316--UO ₂ (20%) Powder Compact -- Sintered, Pressed and Resintered	54
Fig. 3.8	Clad 316--UO ₂ (20%) Powder Compact -- Sintered and Rolled	55
Fig. 3.9	Clad 316--UO ₂ (20%) Powder Compact -- Sintered, Rolled and Resintered	55
Fig. 3.10	Double Clad 316--UO ₂ (20%) Powder Compact -- Sintered, Pressed and Resintered	56
Fig. 3.11	Double Clad 302--UO ₂ (30%) Pressed Compact -- Hot Rolled 90%	56
Fig. 3.12	Double Clad Iron--UO ₂ (30%) Pressed Compact -- Hot Rolled 54%	58
Fig. 3.13	Double Clad Iron--UO ₂ (30%) Pressed Compact -- Hot Rolled 88%	59
Fig. 3.14	Double Clad Iron--UO ₂ (50%) Pressed Compact -- Hot Rolled 78%	59
Fig. 3.15	Screens -- Electroformed and Punched	61
Fig. 3.16	Single Crystal Sphere of Copper Electrolytically Etched, [100] Axis Normal to Page	69
Fig. 3.17	Single Crystal Sphere of Copper Electrolytically Etched, [111] Axis Normal to Page	69

LIST OF TABLES

Table 1.1	Shear Modulus of Thorium	16
Table 2.1	X-ray Diffraction Specimen Data	20
Table 2.2	Effect of Heating on Strength of Cu-U Bonds	37
Table 3.1	Materials Tested in Sodium at 1000°C	39
Table 3.2	Materials Tested in Lead at 1000°C	45
Table 3.3	Materials Tested in Bismuth - Uranium Alloy at 1000°C	47
Table 3.4	Data on Thermal Convection Loops Operated by ANP Experimental Engineering Group	48
Table 3.5	Data on Loops in Operation or Being Examined Metallographically	49
Table 3.6	Information on Loops Being Constructed	49
Table 3.7	Compatibility Test Data	63

SUMMARY

Research on the metallurgy of thorium and on fabrication techniques has continued. The stability and corrosion resistance of thorium exposed to eutectic NaK is being investigated. Extrusion as a means of fabrication of thorium tubes or rods is under study. Experience thus far indicates that a satisfactory product can be produced. Rolling and swaging thorium presents no great difficulty, thorium being similar to uranium in this respect. Drawing, however, has been unsuccessful. This may be the result of too high a drawing speed, and a new variable-speed drive is being installed on the draw bench so that slower speeds may be obtained. A sample of iodide-process thorium has given strain-hardening values about half those of Ames thorium. Work has been started to determine the shear modulus of thorium.

The fabrication of uranium tubing by extrusion has shown that success can be obtained in the alpha range but not in the gamma range. The study of preferred orientations in uranium by X-ray diffraction using a spherical specimen has been continued for extruded uranium. Increasing the extrusion ratio resulted in an increase in the strength of the [410] fiber texture with respect to that of the [010] component with increase in sharpness of both; from front to back end of the extruded length the relationship was reversed.

Work is continuing on the behavior of elementary metals and commercial alloys in liquid-metal media. Metallographic examination rather than weight change or solubility measurements is being depended on to a great extent to determine the nature and extent of attack. A re-evaluation of previous static-corrosion results gained with a three-component system (container, sample, and media, where the container is different from the sample) has been started using a two-component system (container and sample same). Thermal convection loops of various materials containing sodium, lead, or lithium have been or are being run. Twenty-two contain sodium, eight contain lead, and two contain lithium. The lack of suitable welded joints has thus far limited the service life of Na-filled thermal convection loops.

The equipment for the powder metallurgy laboratory is arriving steadily, and is being installed with as little delay as possible. Work on units suitable for incorporation into a solid-fuel element for a high-temperature reactor has begun. A plate that could be used either as made or fabricated into a tube is under development. This plate is to have the following characteristics:

1. A layer of UO_2 must be held in a metallic matrix.
2. The fuel layer must be clad on one side or both sides.
3. The fuel layer is to be approximately 0.005 in. thick and the cladding 0.010 in. thick.

Three methods of fabrication for such a plate have shown promise:

1. Filling the holes in a perforated metal plate with UO_2 and cladding the plate.
2. Sintering a loose powder to a plate.
3. Using a powder compact and cladding with a technique similar to that used in producing MTR plates.

The compatibility testing of potential fuel element materials has continued.

The installation of the creep-rupture and welding laboratories has continued at a good pace. If equipment delivery schedules are met, both laboratories should be ready for operation in the near future. Some work of a service nature has been done by the Welding Group.

A fundamental study of the corrosion of large single metal crystals by liquid metals has been undertaken. The single crystals will be machined into spheres and then, after careful preparation, will be immersed in liquid metal. This will allow a simultaneous study of the attack of a liquid metal on all possible crystal faces. By this method it is hoped to gain some understanding of the fundamental physicochemical processes involved in liquid-metal corrosion.

I. THORIUM RESEARCH

THEMAL CYCLING OF THORIUM

Samples of thorium in the form of rods $\frac{3}{8}$ in. in diameter and 4 in. long were prepared for thermal cycling in eutectic NaK in order to investigate the stability and corrosion resistance of thorium under these conditions. The samples were measured in all dimensions with micrometer calipers and weighed prior to cycling. After each 100 cycles between 100 and 500°C the specimens will be removed and inspected for dimensional or weight changes. Four specimens are supported in a stainless steel holder and submerged in the liquid NaK which is contained in a stainless steel tank. A high-frequency induction coil around the steel container heats the entire assembly to 500°C and holds the temperature constant for 15 min to ensure uniform specimen temperature. At the end of the holding period the induction heating unit automatically turns off, and air jets are turned on for rapid cooling to 100°C, at which time the air jets are interrupted and power is applied to reheat the container. Since this method of cycling requires that the liquid metal be heated and cooled as well as the test specimens, only one cycle per hour is possible at the present time. A furnace has been designed in which a much faster rate of cycling is to be accomplished by maintaining two constant-temperature baths and alternately submerging the rack of specimens in the hot and cold NaK.

METALLOGRAPHY OF THORIUM

Considerable difficulty has been experienced in satisfactorily etching thorium to show the grain boundaries. The most commonly used etch is 50% glacial acetic acid and 50% orthophosphoric acid. A new technique has been developed for bringing out the grain boundaries.

An unmounted specimen was hand-ground through a series of fine abrasive papers from 180 to 600 grit. It was then polished with a silk cloth mounted on a motor-driven polishing disk. Medium-fine alumina powder was used to remove the grinding scratches caused by the papers. For the final polishing, the specimen, used as the anode, was suspended, by a stainless steel clamp, vertical to the stainless steel cathode for 3 to 5 sec in an electrolyte consisting of 1 part of perchloric acid and 10 parts of glacial acetic acid. The short time used allowed slight metal removal with little attack on inclusions.

The cathode-anode distance was about 3 in., the voltage was 50 volts, and the current density was 4 amp/in.² The specimen was removed from the cell with the current on and was immediately immersed in a small amount of fresh electrolyte to remove a loose film formed during electrolysis.

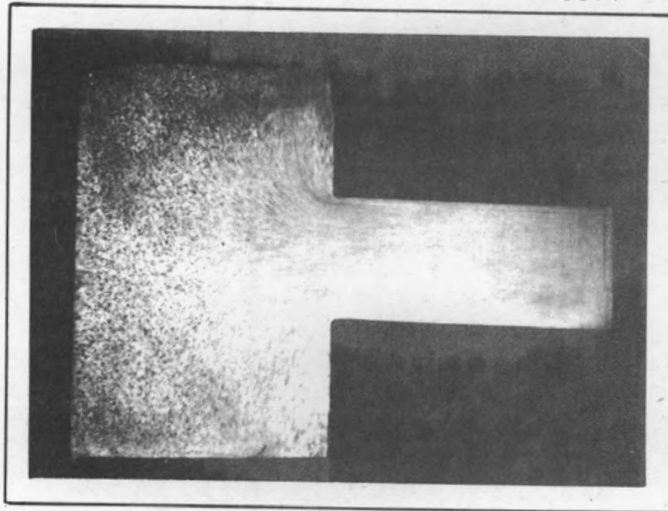
Because of the etching effect of the polishing electrolyte, examination was made without further etching.

FABRICATION OF THORIUM

Extrusion. Extrusions have been made from four cast, unclad billets of Ames thorium. The experience gained with these extrusions indicates that a satisfactory product can be extruded as the initial step in the fabrication of either rods or tubing. The surfaces of the extruded specimens were rough, but spots of smooth surface along the rod showed some good flow. This indicates that the production of smooth surface is a matter of extrusion technique. A sample cut from the center of a 1-in.-O.D. by 3/8-in.-I.D. tube of extruded thorium is shown in Fig. 1.1B; a photomicrograph of this sample is shown in Fig. 1.1C.

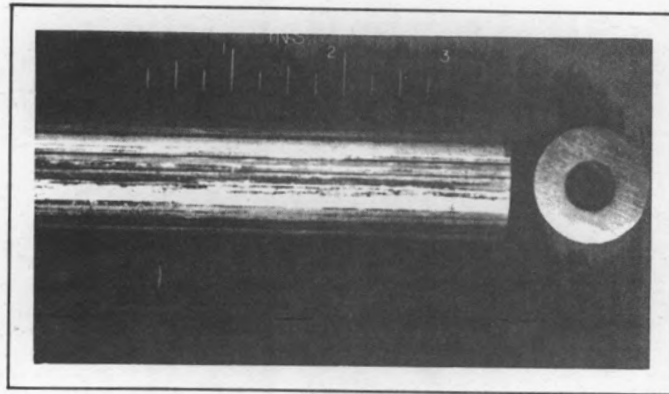
The conditions used for extrusions of the thorium rod and tubing were as follows:

Heating medium for the billet	Salt bath 950°C (Liquid Heat N.D.)
Billet heating time	1 hr
Billet size (rod)	2-15/16 in. diameter by 3½ in. long
Billet size (tubing)	2-15/16 in. O.D. by 9/16 in. I.D. by 3½ in. long
Reduction ratio (rod)	8.93 to 1
Reduction ratio (tubing)	10.22 to 1
Extrusion speed	Approximately 25 ft/min
Extrusion starting pressure	Approximately 40 tons/in. ² on billet
Container temperature	400°C
Die temperature	600°C
Die type	1-in.-diameter throat, flat face, insert (insert made of "Doss Steel Research" 3130)
Lubricant for tubing	15% lampblack—85% beeswax on mandrel and die face



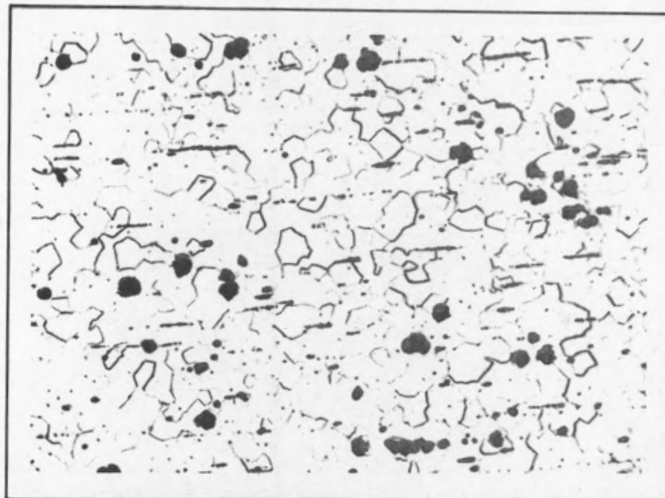
Y-2987

PARTIAL EXTRUSION OF THORIUM



Y-3078

TUBE EXTRUSION OF THORIUM



ETCH: GLACIAL ACETIC, Y-3092
PERCHLORIC ACID.

225X

PHOTOMICROGRAPH OF EXTRUDED TUBE
EXTRUDED THORIUM

FIG. I.I

Since the considerable erosion that occurred with a die face of Latrobe LPD steel indicated that the metal was flowing across the flat face of the extrusion die, a billet was partially extruded and sectioned to study the flow characteristics; the removed portion was approximately 6 in. long (see Fig. 1.1A). This partial extrusion indicates that the billet as a whole moves down the container somewhat and that most of the flow takes place in the vicinity of the die.

Further study of die design and lubricants will be carried out to improve surface condition of the extruded shape.

Rolling and Swaging. Several pieces of thorium rod have been rolled and then cold swaged with a total reduction of approximately 70% without any difficulty. Thorium rolls and swages somewhat like uranium.

Drawing. Three attempts have been made to draw $\frac{1}{2}$ -in.-diameter thorium rods without success. The rods were swaged to a diameter 0.005 in. larger than the drawing die, annealed, coated with lubricant, and then drawn. The lubricants used were "Molykote" (molybdenum sulfide), 3 parts of "Flintcote" 715 to 1 part of "Motor Mica," and "Fluorthene." All the samples appeared to draw satisfactorily, but when these rods were then drawn through a die 0.010 in. smaller in diameter, seizing occurred after approximately 4 in. or less had gone through the die.

The draw bench is a 10-ton unit with a fixed speed of 40 ft/min which was salvaged from other work. Replacement of the drive in order to permit speeds from 0 to 40 ft/min is now in progress. Since the drawing speed is one of the major factors in satisfactory drawing, further work will be held up until the new drive is installed.

WORK HARDENING OF IODIDE-PROCESS THORIUM

A small ingot of thorium prepared by the iodide process at Battelle Memorial Institute has been received. Details of preparation and chemical analysis of the ingot are not yet available; however, it is likely that the iodide-process thorium is considerably purer than other thorium samples which have been used in this research.

At Oak Ridge National Laboratory the ingot of iodide-process thorium was rolled slightly and vacuum annealed at 700°C. The specimen was then further

reduced by cold rolling, and the effect of cold reduction on hardness was determined. The iodide-process thorium rolled easily, and one specimen was rolled to a thickness of 0.001 in. (99.5% reduction) without any evidence of cracking.

The effect of cold rolling on the hardness of the iodide-process thorium is shown in Fig. 1.2. Plotted points represent the average of five measurements. A 5-kg load was used for most of the hardness tests, a load of 1 kg being used for tests on the thinnest specimens. Similar data previously obtained on samples of Ames thorium are also shown in Fig. 1.2.

RECRYSTALLIZATION OF THORIUM

Recrystallization studies of cold-worked thorium were continued. Specimens of cold-rolled thorium sheet were annealed for definite time intervals in a lead bath maintained at the desired temperature, and the extent of recrystallization was determined from hardness measurements.

Typical recrystallization curves obtained from specimens of Ames thorium cold rolled to 80% reduction in thickness are shown in Fig. 1.3. From these data it appears that the rate of recrystallization of this thorium is considerably greater at temperatures of 550°C and above than it is at temperatures of 535°C or lower.

Additional recrystallization tests are in progress. These experiments are intended to define the effects of impurities and amount of cold working on the rate of recrystallization.

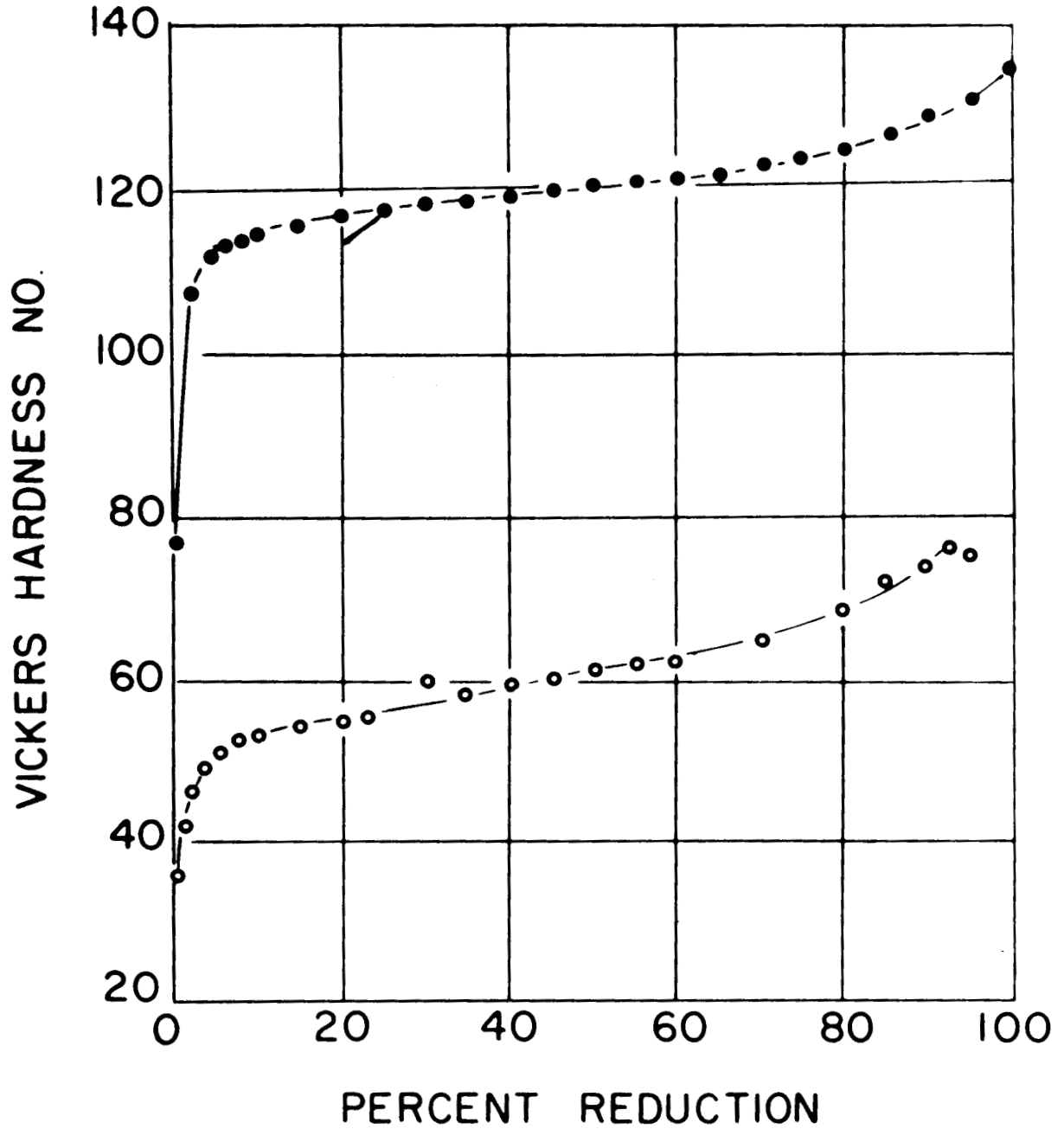
SHEAR MODULUS OF THORIUM

Some preliminary tests were made to determine the shear modulus of Ames thorium rods. A simple torsion-test machine was used. One end of the test specimen was fixed by clamping in a stationary chuck, the other end being clamped in a chuck mounted in freely rotating bearings. Torque was applied to the rotating chuck through a weight-loaded lever arm. A dial indicator actuated by the lever arm provided for measurements of twist. Test specimens were 0.590 in. in diameter with a gauge length of 4.72 in.

Y-3148

• - AMES THORIUM

○ - IODIDE THORIUM



STRAIN HARDENING CURVES FOR AMES AND IODIDE THORIUM

FIG.1.2

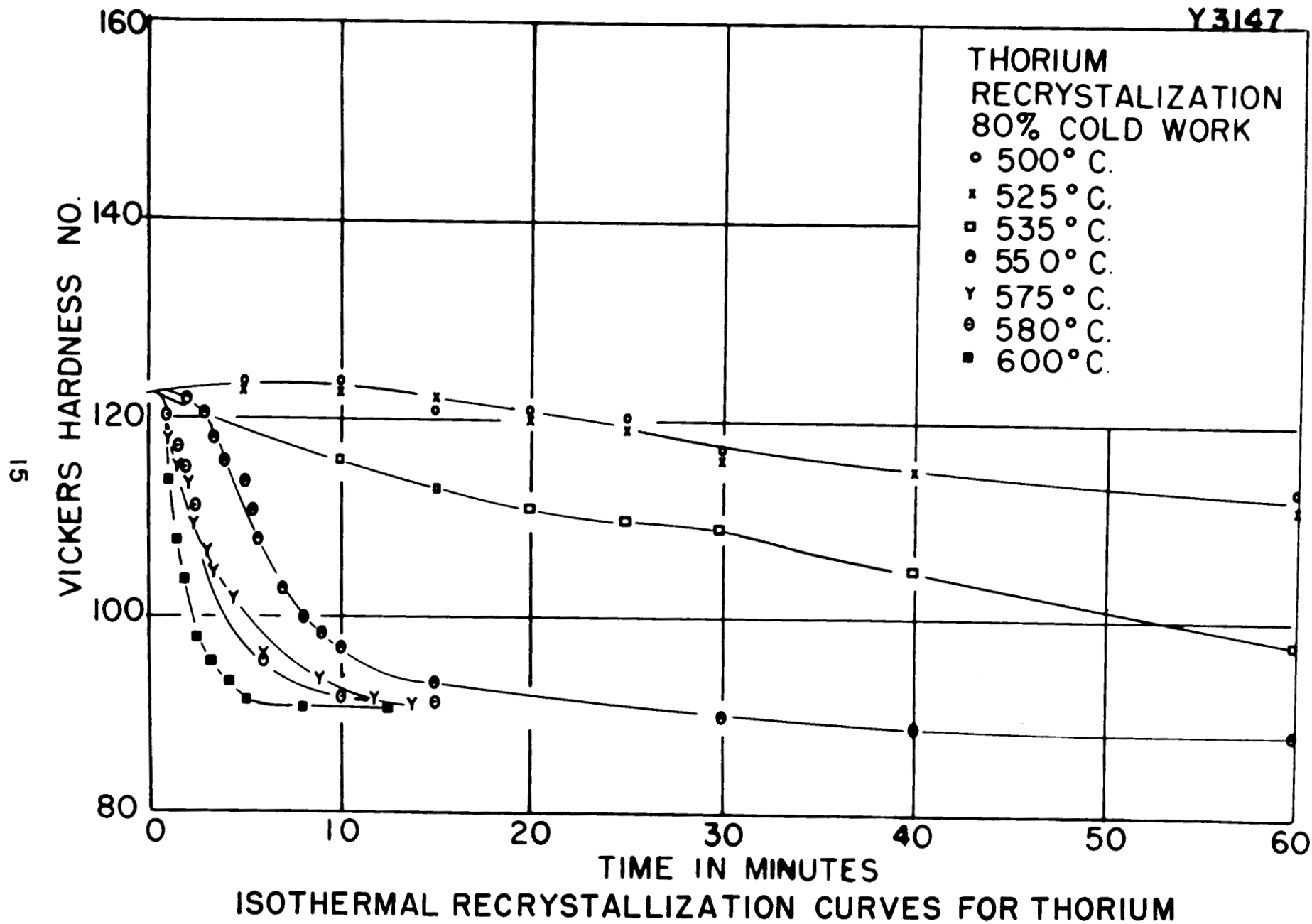


FIG. I.3

Results of torsion tests to determine the shear modulus of three specimens of thorium together with results of tests on ingot iron and aluminum specimens are shown in Table 1.1. From these data it appears that the experimental values may be slightly low, which may be the result of slight movement of the fixed chuck of the machine. These values of shear modulus will be checked when a suitable method for determining actual twist in the specimen is available.

TABLE 1.1
Shear Modulus of Thorium

MATERIAL	SHEAR MODULUS (lb/in. ²)	
	EXPERIMENTAL VALUE	HANDBOOK* VALUE
Ingot iron	10,800,000	11,770,000
	10,400,000	
	10,300,000	
Aluminum (2S)	3,560,000	3,850,000
Thorium	4,080,000	
	3,910,000	
	3,890,000	

*Metals Handbook, American Society for Metals, Cleveland, Ohio, 1948.

2. URANIUM RESEARCH

FABRICATION OF URANIUM TUBING

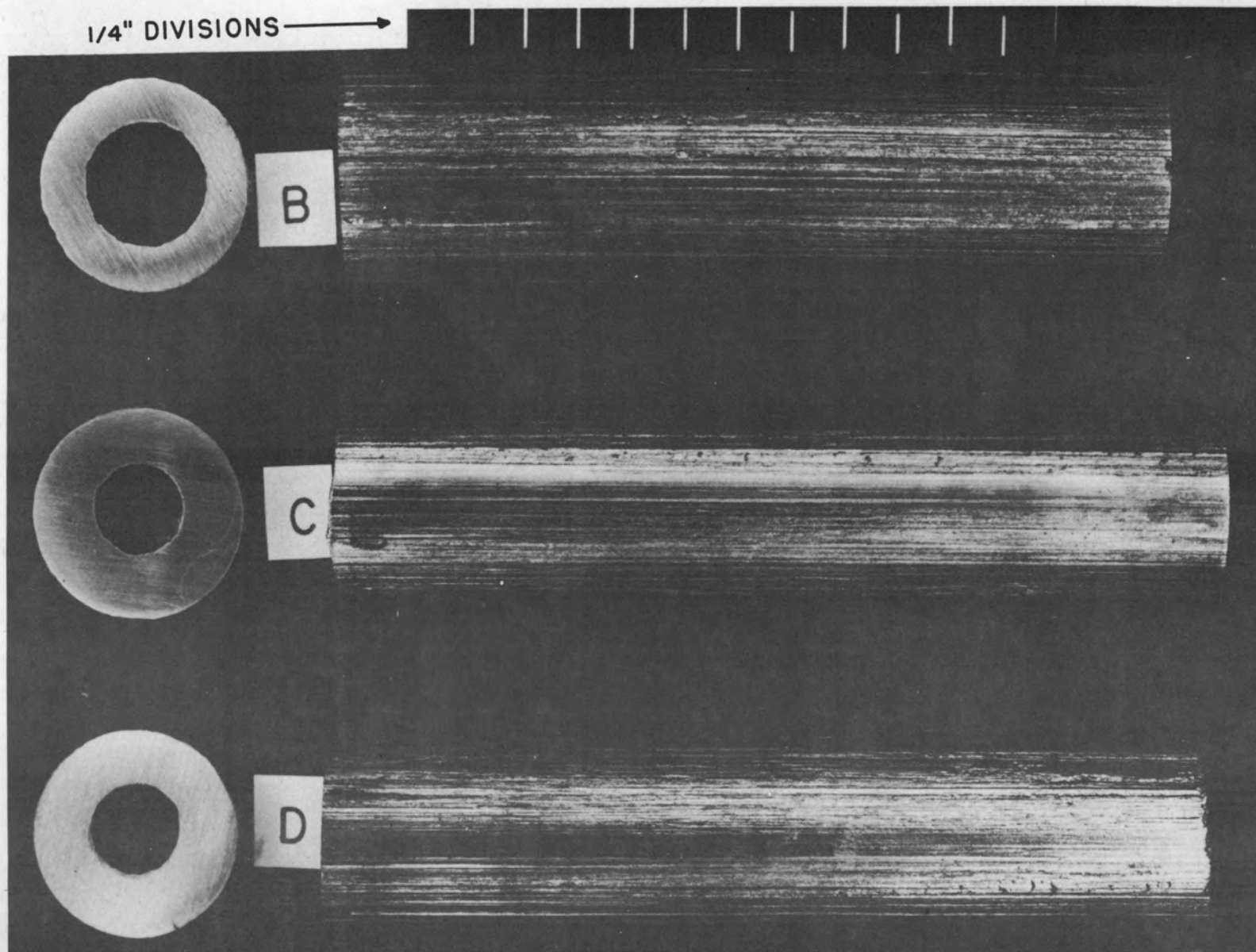
Some work has been done on extrusion of uranium tubing to fill a need at the laboratory. Five attempts have been made to extrude 1-in.-O.D. tubing with 3/8- and 1/2-in. bores. The extruded tubing was spray quenched with water as it left the die, and the main difficulty was oxidation of the inside of the tube bore because of inadequate cooling. Two tubes were extruded in the gamma range (900°C) without appreciable success, but successful extrusions were made in the alpha range (550°C). Typical sections of the tubing are shown in Fig. 2.1. Although the samples appear quite rough in the photograph, owing to shadows, the surface was relatively smooth in some areas.

The billets were extruded bare from a bath of boron anhydride after they had been cooled to 550°C. (The boron anhydride was applied by dipping the billets in the bath for 15 min at 900°C.) A 15% lampblack—85% beeswax mixture was used for additional lubrication on both the mandrel and the die. Extrusion speed was of the order of 20 ft/min.

PREFERRED ORIENTATION AND ANISOTROPY IN PROPERTIES OF METALS

A comprehensive investigation has been made of the preferred orientations developed in high- α -extruded uranium rod. Rods 1½, 9/10, and 5/8 in. in diameter were extruded through 25° conical dies from ingots 3-1/8 in. in diameter at 500°C billet temperature (extrusion ratios 4.3, 12.1, and 25.0, respectively). The extruded lengths were water-spray quenched as they emerged from the die to retain, in so far as possible, the as-extruded structure.

A sample was taken from the front, middle, and back of each extruded length, from which a spherical diffraction specimen 0.500 in. in diameter was machined so that the center line of the specimen coincided with that of the rod, as shown in Fig. 2.2. The spherical surfaces of the specimens were lapped to smoothness and electropolished to remove the surface layers deformed by machining and lapping (the specimens were reduced in diameter approximately 0.010 in. by electropolishing). The specimens are identified in Table 2.1.



18

ALPHA EXTRUDED URANIUM TUBING

FIG. 2.1

NOT CLASSIFIED

EXTRUSION
DIRECTION

DWG. 10948
~~CONFIDENTIAL~~

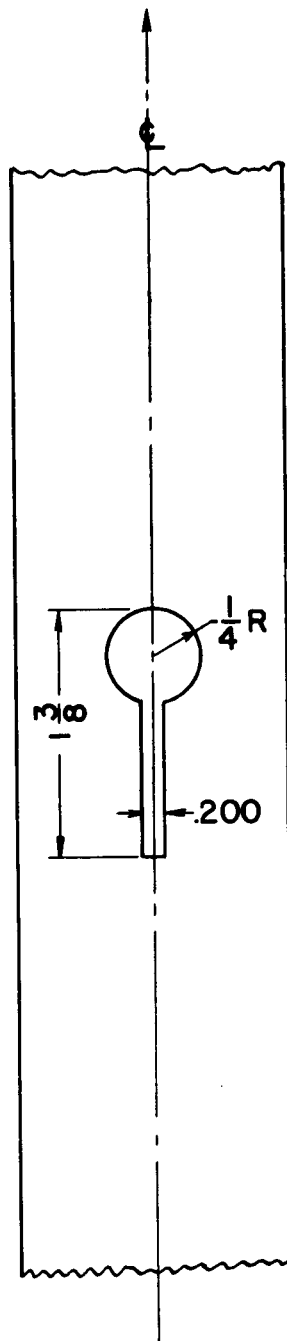


FIG. 2.2

SKETCH SHOWING THE DIMENSIONS OF THE X-RAY
DIFFRACTION SPECIMENS AND THE LOCATION IN THE
SAMPLE OF α -EXTRUDED URANIUM ROD FROM WHICH
THEY WERE MACHINED.

TABLE 2.1
X-ray Diffraction Specimen Data

SPECIMEN NO.	DIAMETER OF EXTRUDED ROD (in.)	EXTRUSION RATIO	LOCATION* IN EXTRUDED LENGTH
U9-11 - 5 - 12	1½	4.3	Front Middle Back
U10-13 - 14 - 15	9/10	12.1	Front Middle Back
U12-16 - 17 - 18	5/8	25.0	Front Middle Back

*Front = ¼, middle = ½, and back = ¼ distance along extruded length.

The preferred orientations were determined by the X-ray diffraction spectrometer technique described in previous reports.^(1,2) Examination was made on a Norelco Type 12021 Geiger counter X-ray diffraction goniometer employing Cu K α radiation. The specimen was rotated at 200 rpm about its longitudinal axis (the extrusion direction) during exposure.

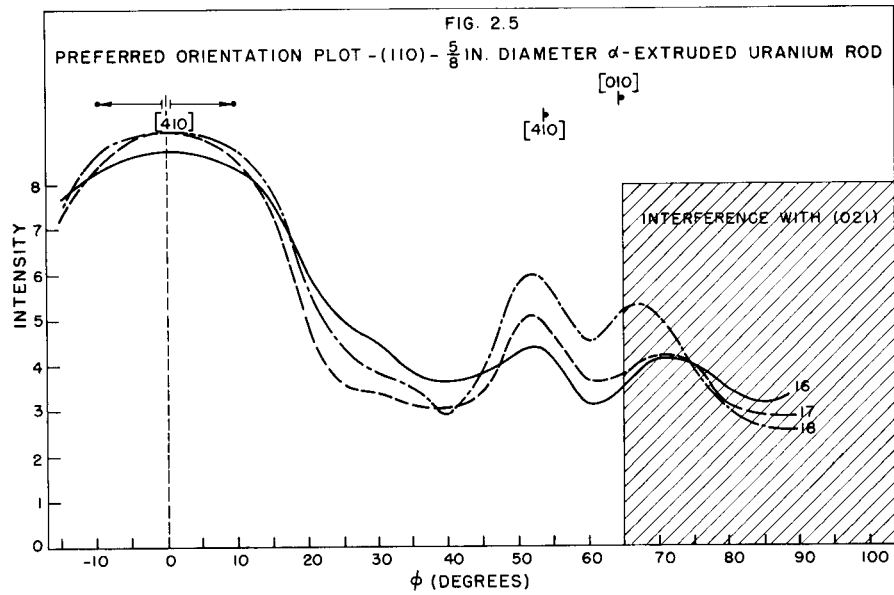
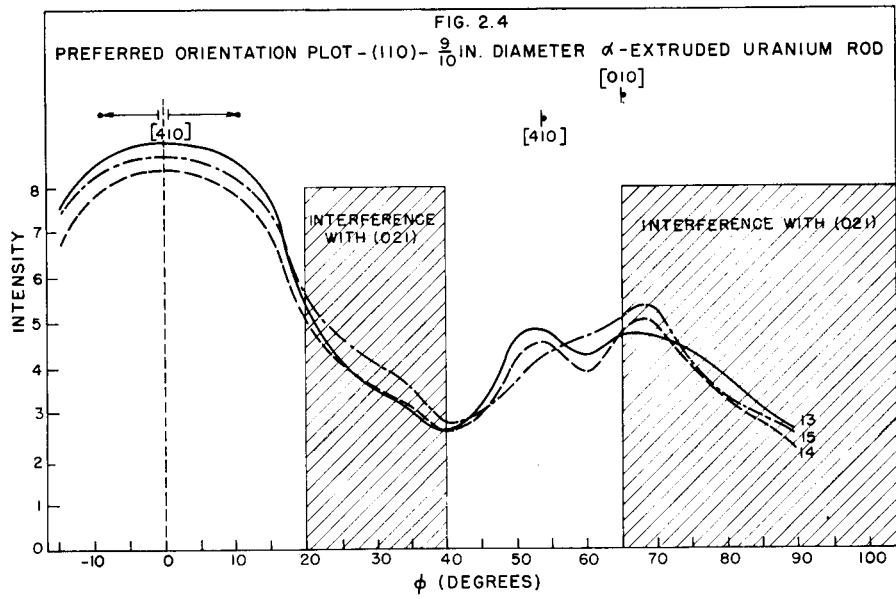
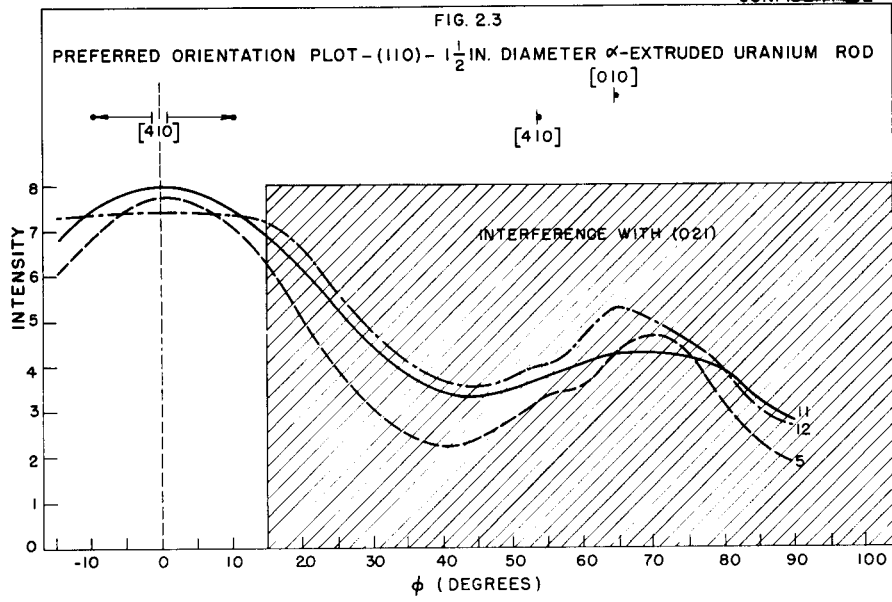
Plots of the intensity of diffraction vs. the angle, ϕ , between the extrusion direction and the normal to the diffracting plane for various planes for each specimen are given in Figs. 2.3 to 2.29.

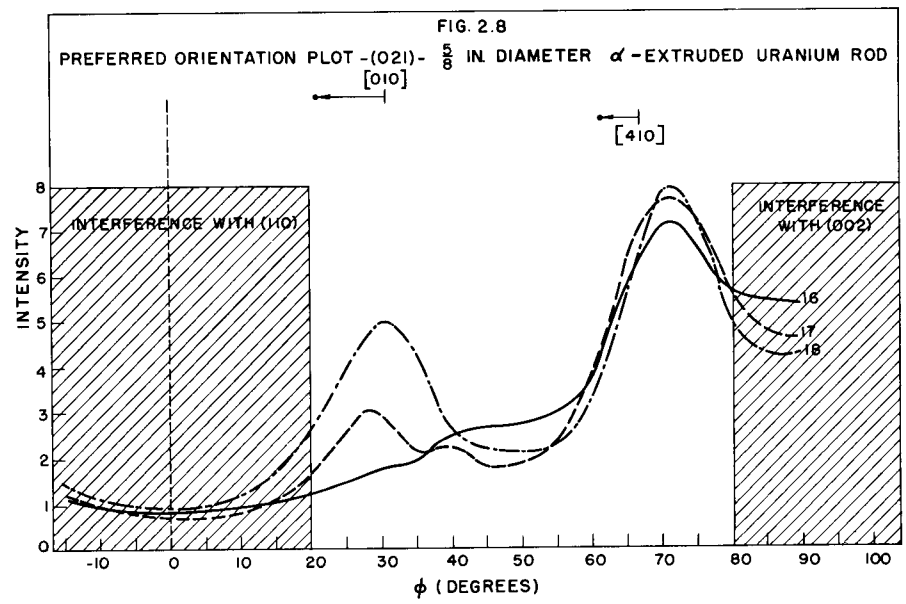
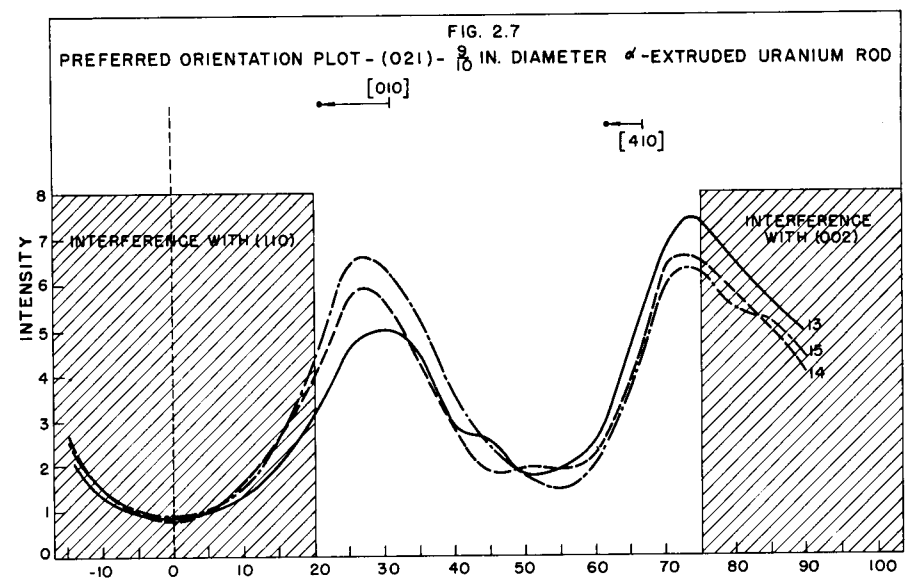
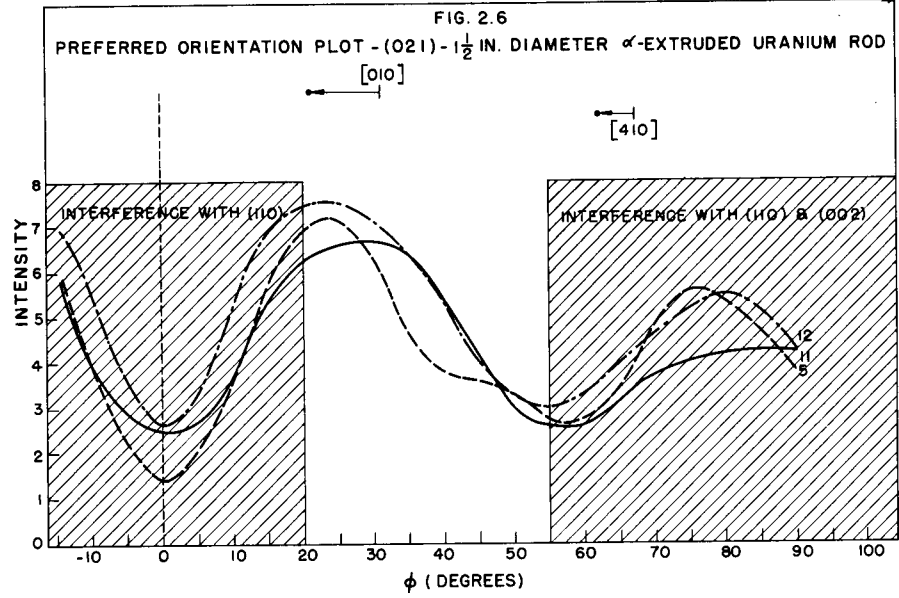
Analysis of the data revealed the following features of the preferred orientation in these α -extruded uranium rods and the changes brought about by certain fabrication variables:

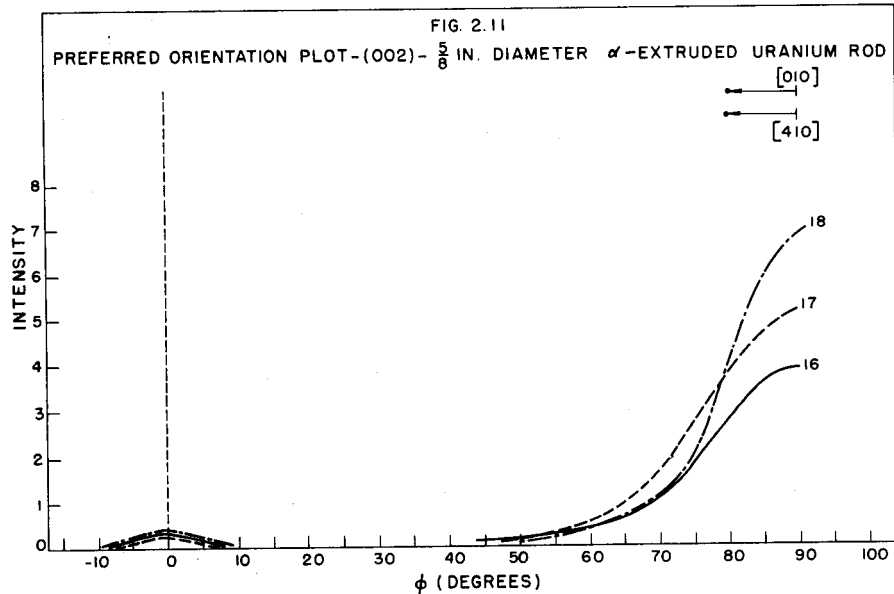
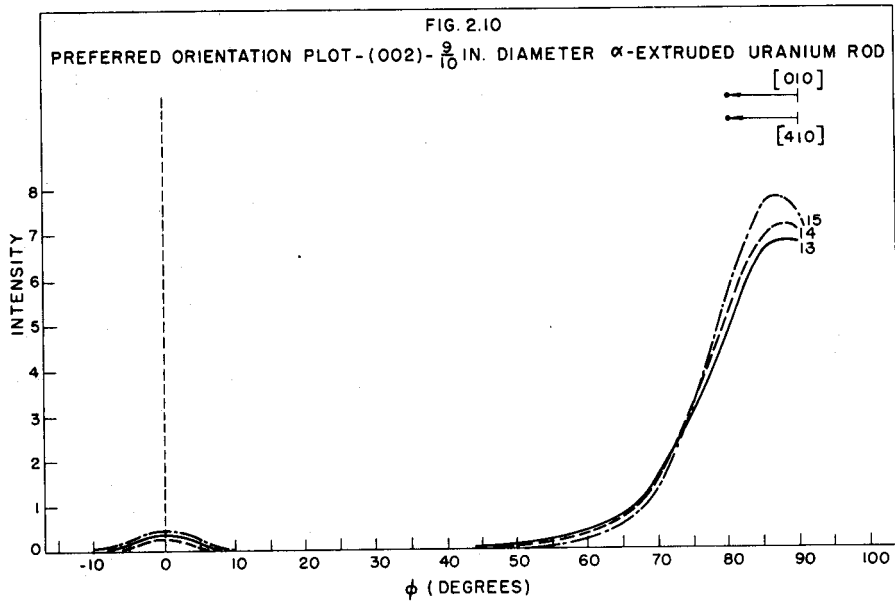
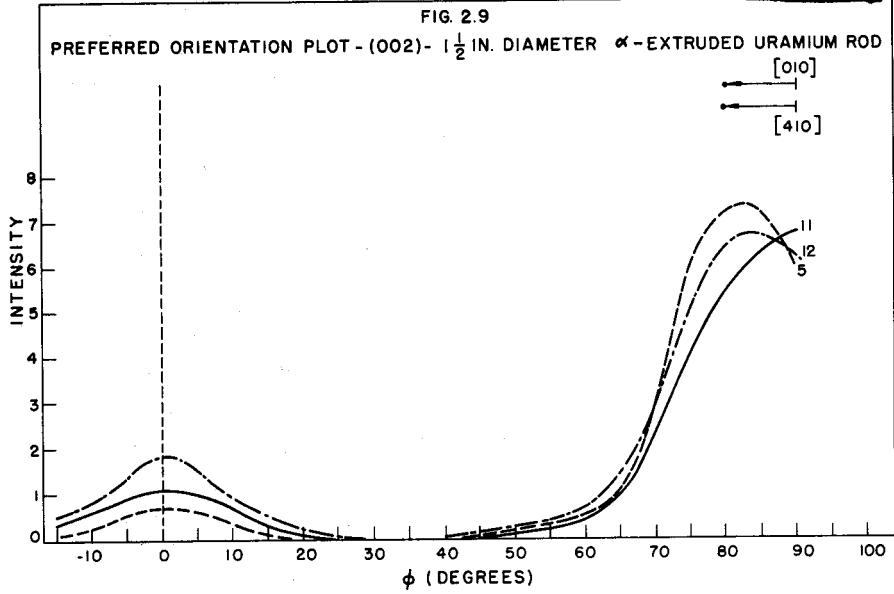
All samples exhibited a duplex [010]-[410] fiber texture. On the graphs in Figs. 2.3 to 2.29 are indicated the positions of the intensity maxima to be expected for the various diffracting planes for these preferred directions. Lack of exact coincidence may be explained by (a) interference with other planes diffracting to nearly the same 2θ values, as indicated; (b) inclination of the preferred directions to the extrusion direction resulting from the development of a zonal or conical fiber texture to be expected for extrusions

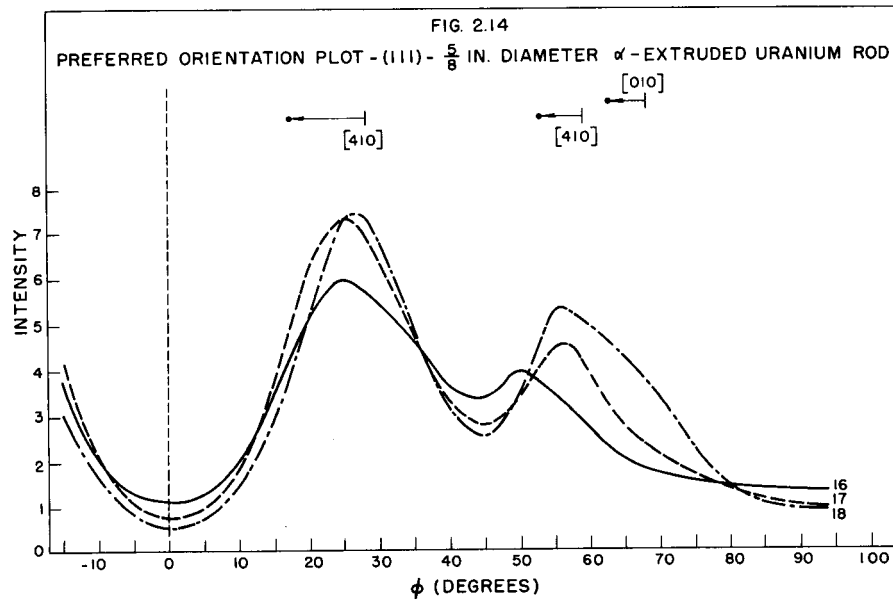
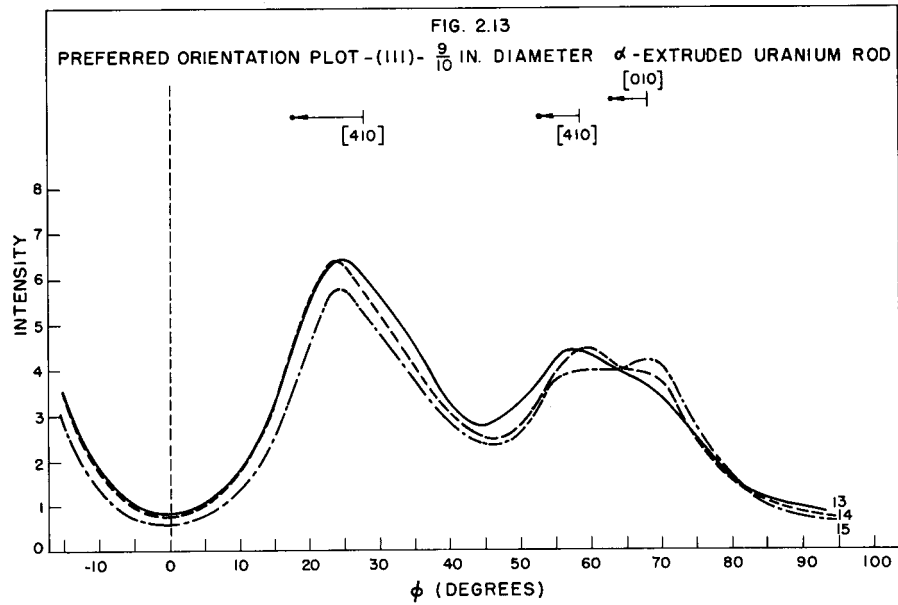
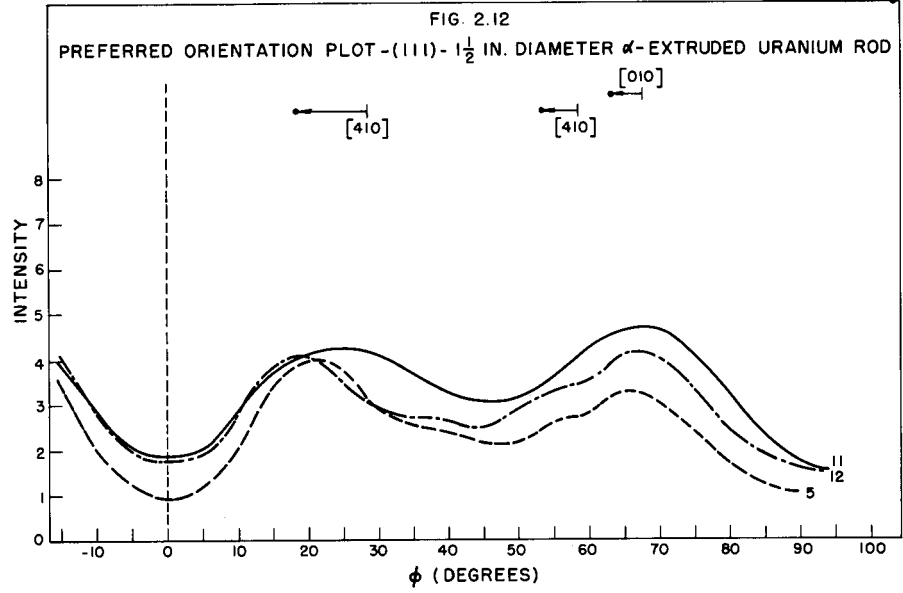
(1) *Metallurgy Division Quarterly Progress Report for Period Ending January 31, 1950*, ORNL-583, p. 37 (Mar. 10, 1950).

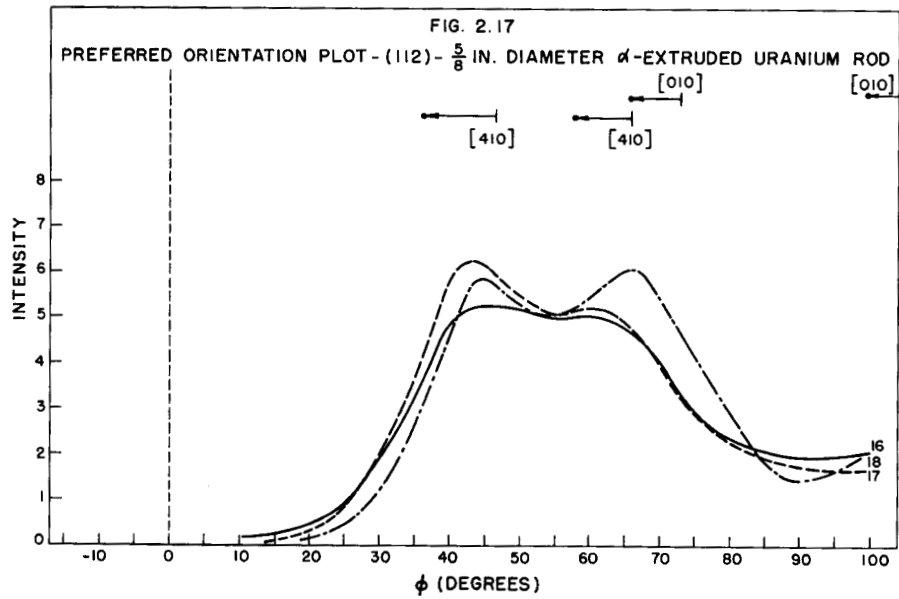
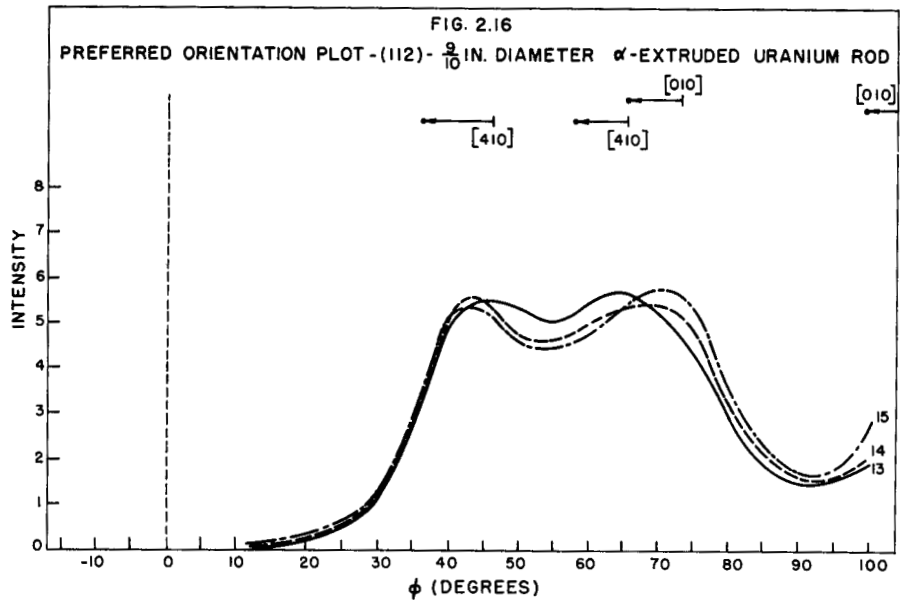
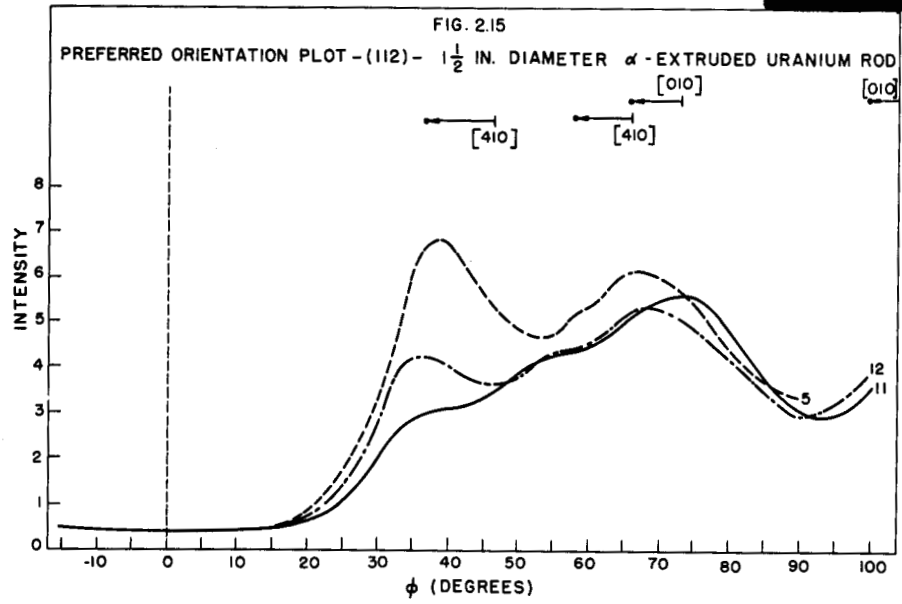
(2) *Metallurgy Division Quarterly Progress Report for Period Ending July 31, 1950*, ORNL-827, p. 35 (Dec. 4, 1950).

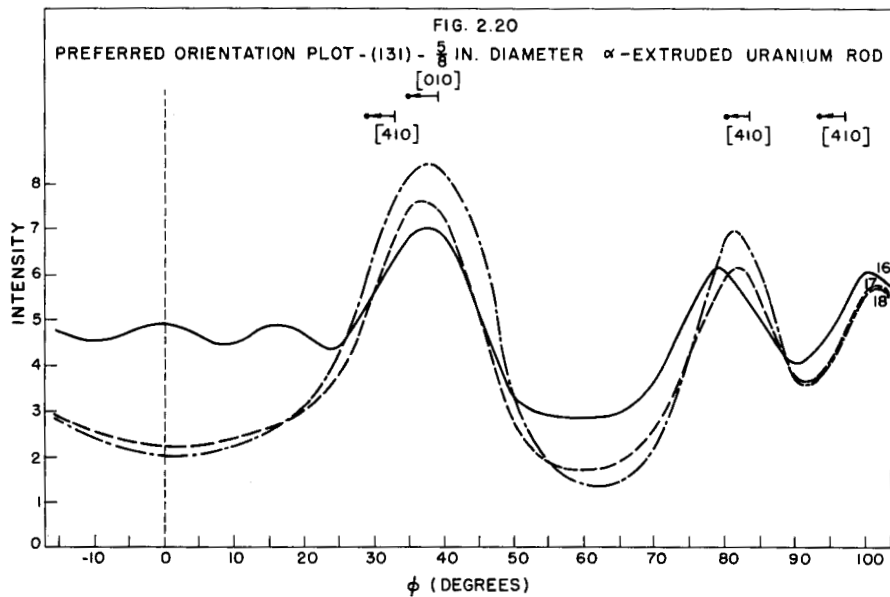
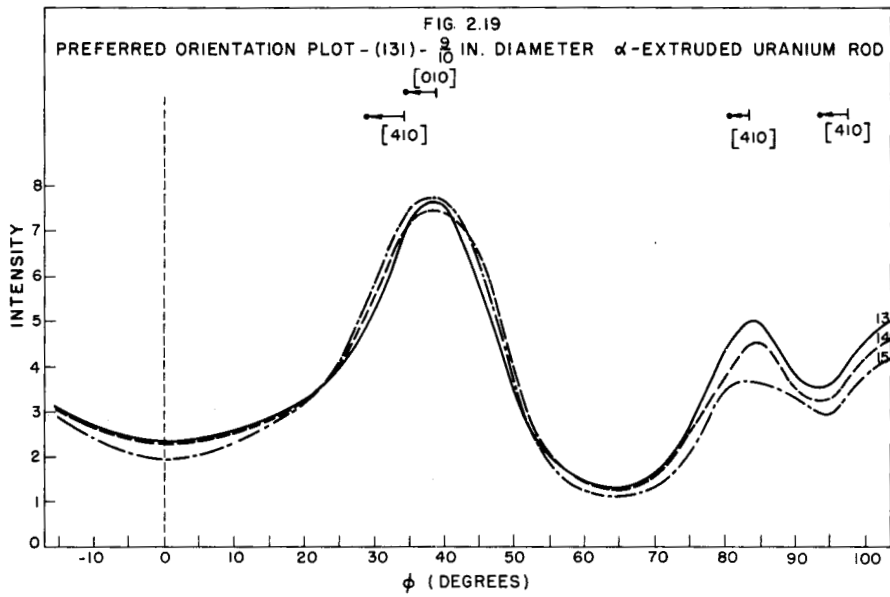
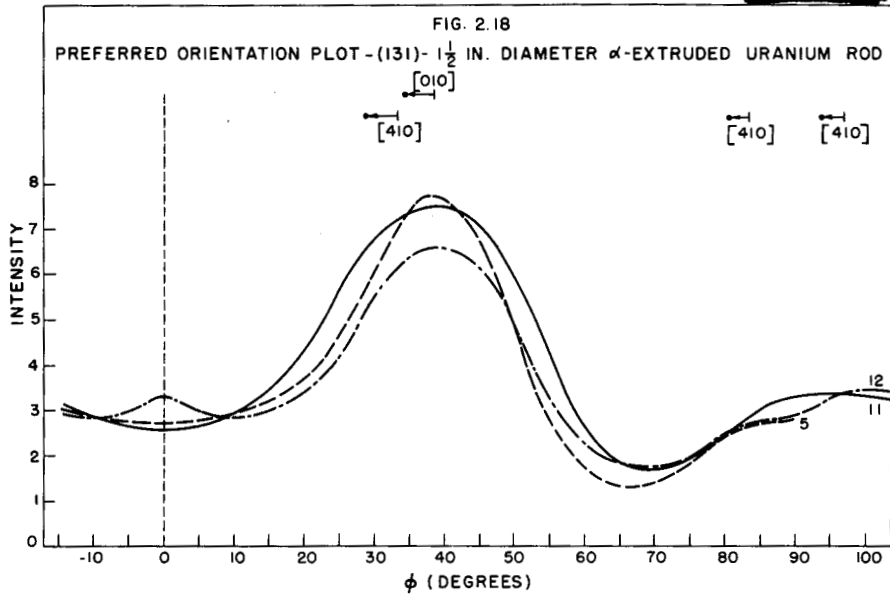


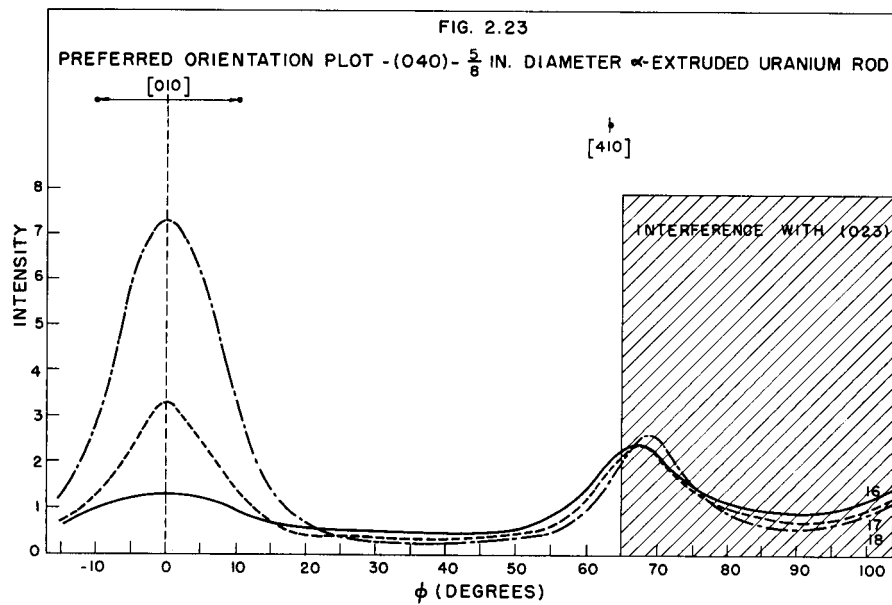
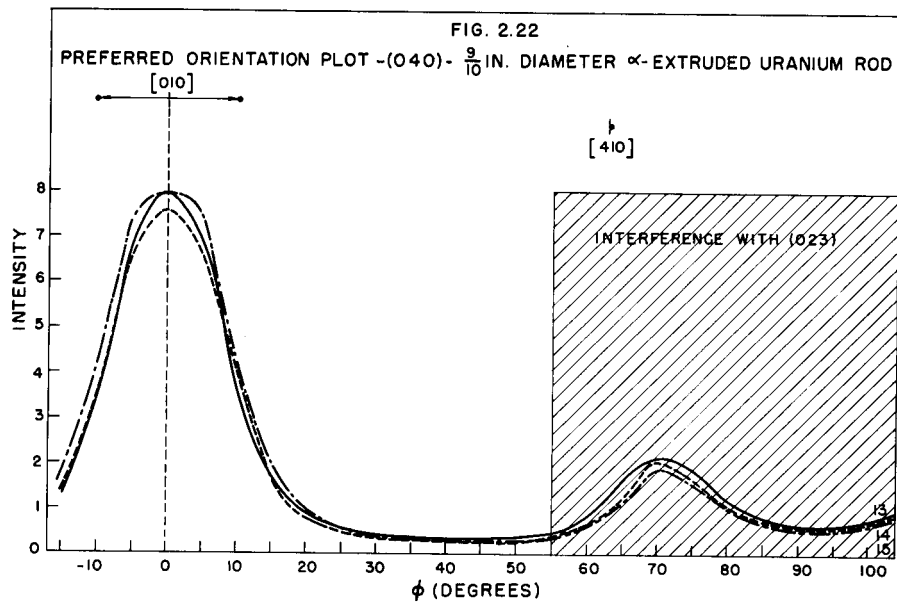
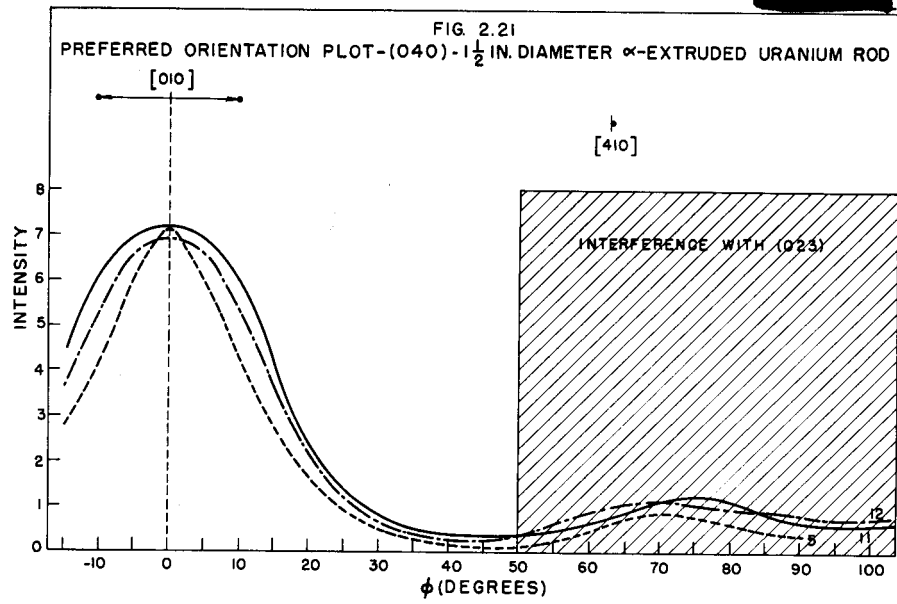


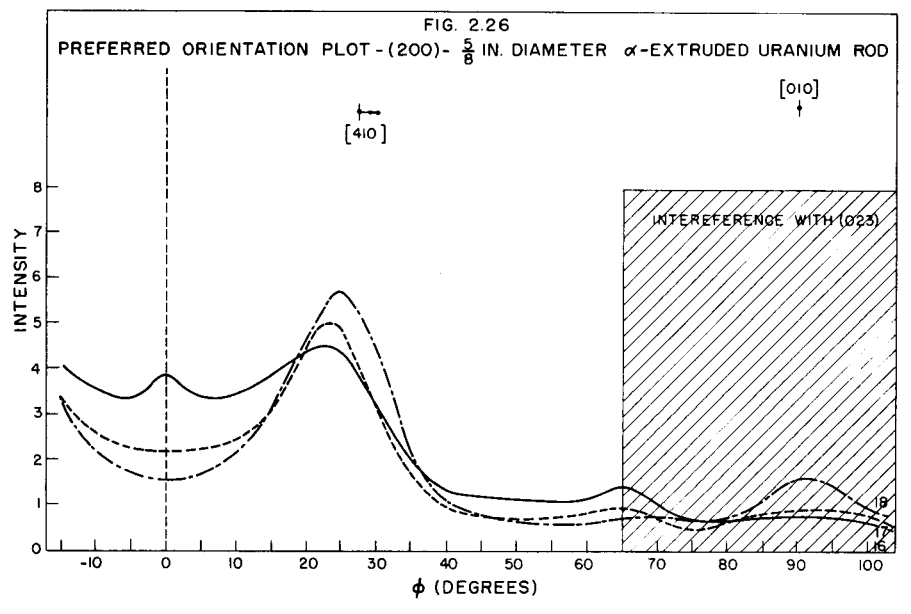
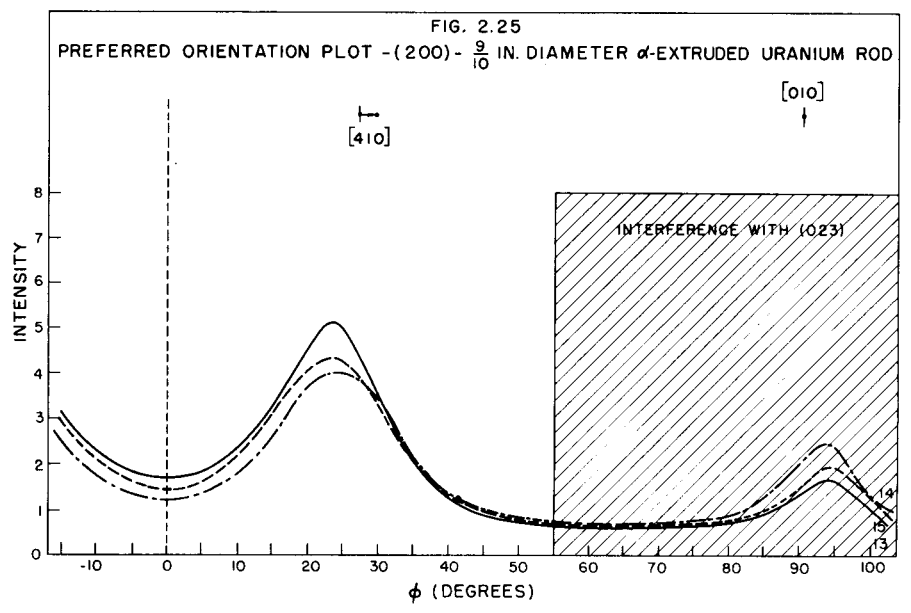
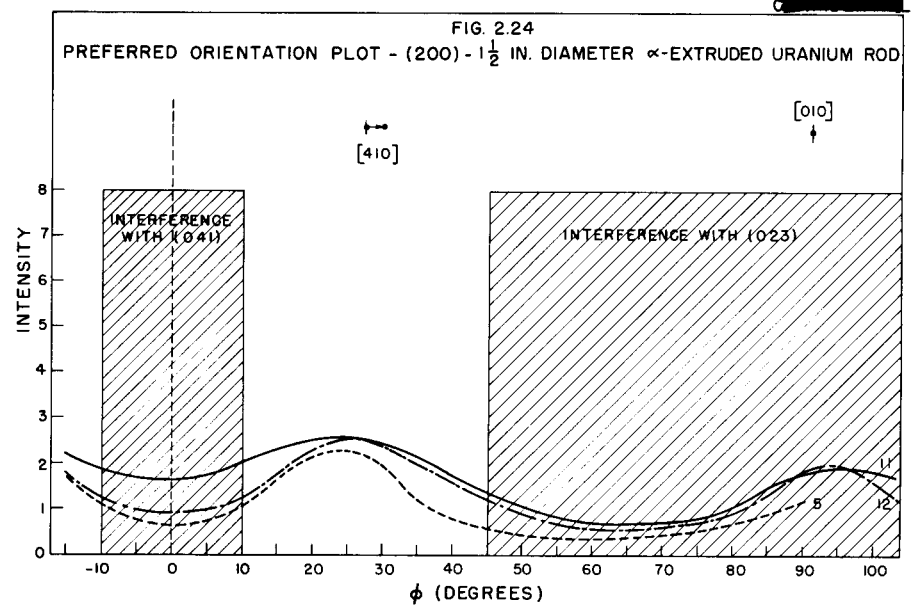


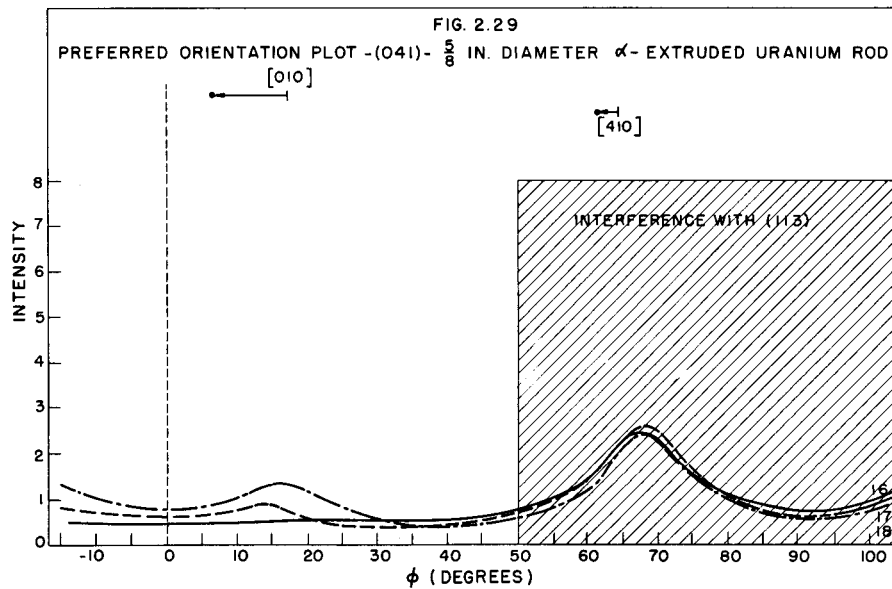
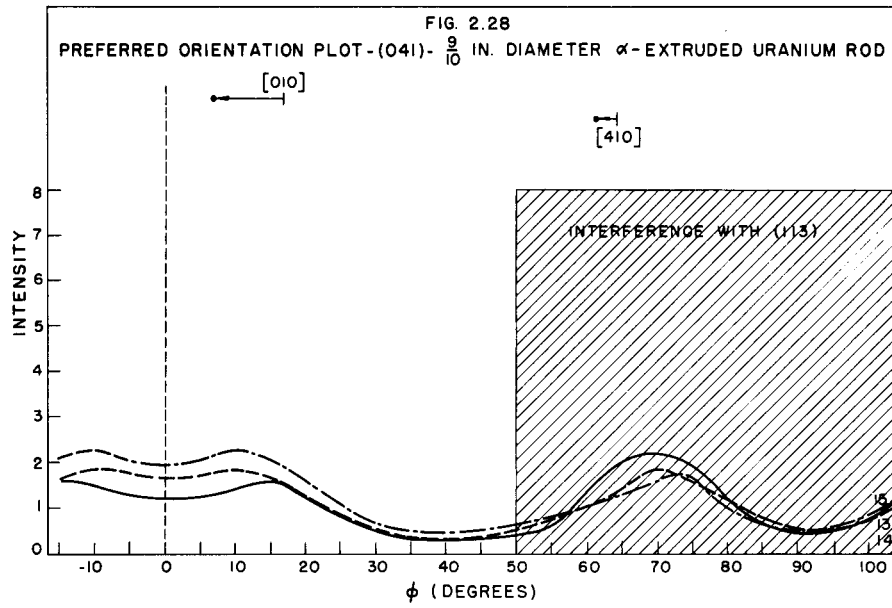
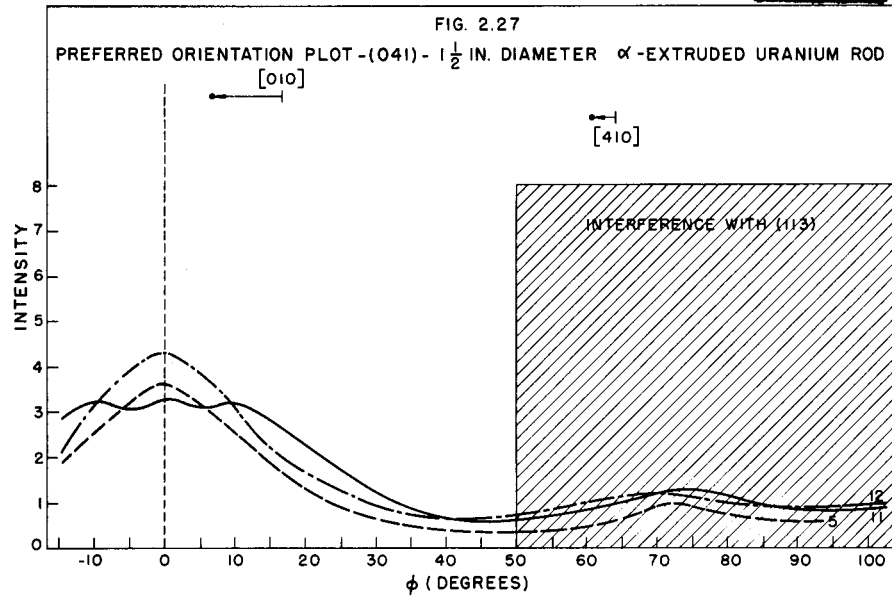












(the shifts in intensity maxima brought about by an inclination of 10° are indicated on the graphs); and (c) influence of certain minor components in the texture, such as [031], [321], [001], and [100].

Increasing the extrusion ratio resulted in an increase in the strength of the [410] relative to that of the [010] component with increase in sharpness of both.

From the front to the back end of the extruded lengths there was an increase in the strength of the [010] relative to that of the [410] component with increase in sharpness of both.

The microstructures of the samples from which the diffraction specimens were taken are shown in Figs. 2.30 to 2.34. They show that the degree of recrystallization increased with increase in extrusion ratio, and, for the rod given the greatest reduction, that the degree of recrystallization decreased from the front to the back end of the extruded length.

It would appear from this that the preferred orientation is related to the microstructure in that, for a deformed structure, with increasing degree of deformation the strength of the [010] increases relative to that of the [410] component; and, for partially recrystallized structures, with increasing degree of recrystallization the strength of the [410] increases relative to that of the [010] component.

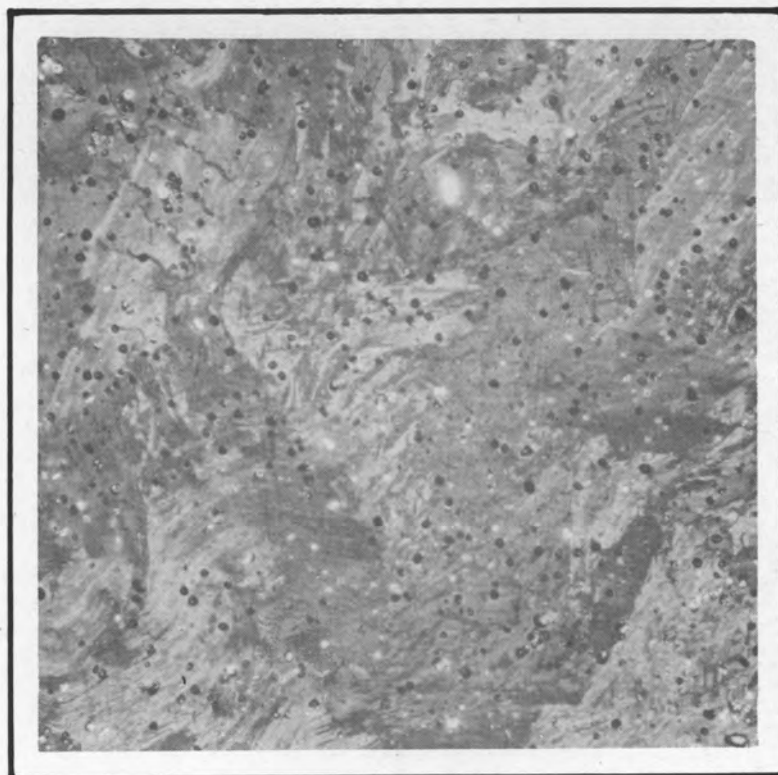
A recent attempt has been made to rationalize the textures of uranium rod fabricated in the α range on the basis that the relative strengths of the [010] and [410] components depend upon the temperature of deformation, the former becoming more prominent with decrease in temperature, and that recrystallization does not change the texture developed by deformation.⁽³⁾

There is a possibility that the differences in the relative strengths of the [010] and [410] components observed in the present investigation may be related to differences in the actual temperature of deformation for the different rods and for different locations in the same rod. On the other hand, the excellent correlation of texture and microstructure suggests very strongly that the relative strengths of the two components depend primarily upon the degree of recrystallization.

(3) "Reactor Materials," *Progress Report No. 47, June, 1950*, Section III, p. 12, KAPL-370 (July 28, 1950).

NOT CLASSIFIED
Y-3886

PHOTO NO. Y-1211
M. SPEC.-780-A
TRANS.



MAG.— 150X
ETCH— POL.LIGHT

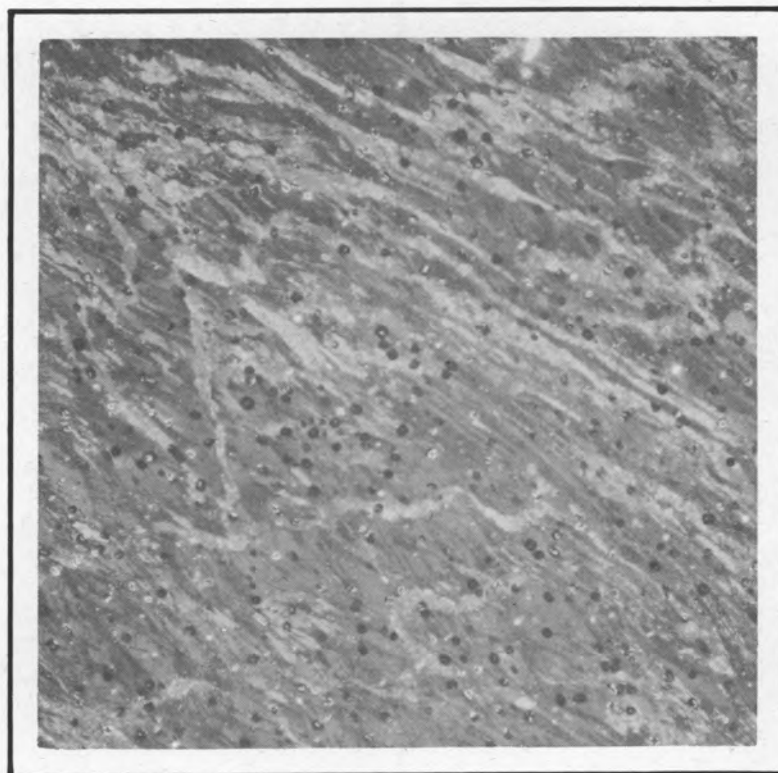


PHOTO NO. Y-1212
M. SPEC.— 780-B
LONG.

PHOTOMICROGRAPHS SHOWING THE DEFORMED GRAIN STRUCTURE
OF THE SAMPLE OF α -EXTRUDED URANIUM FROM WHICH THE X-RAY
DIFFRACTION SPECIMENS WERE MACHINED.

FIG. 2.30

NOT CLASSIFIED
Y-3693

PHOTO NO. Y-1206
M. SPEC.-783-A
TRANS.



MAG.-150 X
ETCH-POL. LIGHT

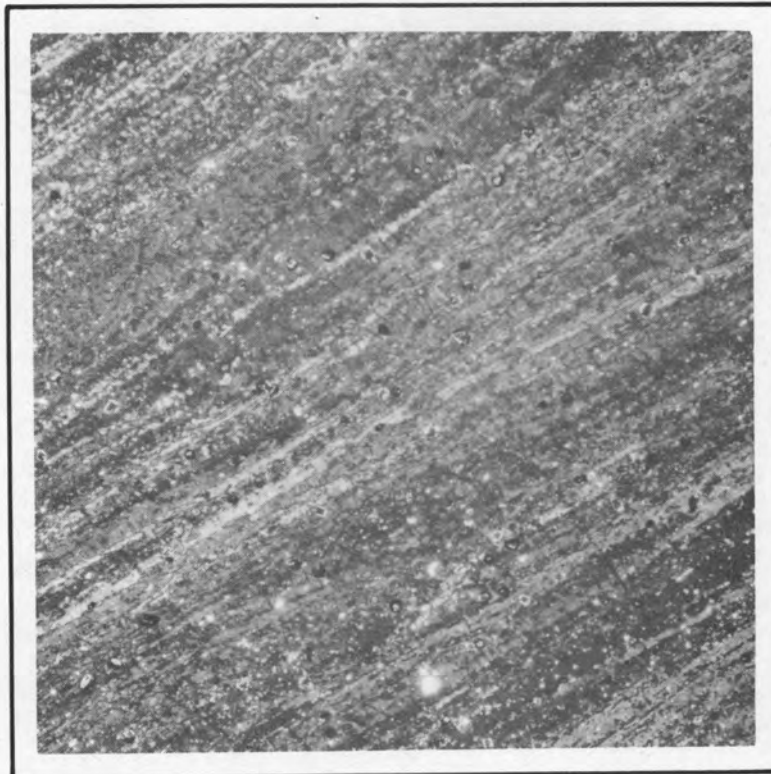


PHOTO NO. Y-1213
M. SPEC.-783-B
LONG.

PHOTOMICROGRAPH SHOWING THE PARTIALLY RECRYSTALLIZED GRAIN STRUCTURE IN THE MIDDLE OF THE LENGTH OF 9/10" DIAMETER α EXTRUDED URANIUM ROD.

FIG. 2.31

NOT CLASSIFIED
Y-3694

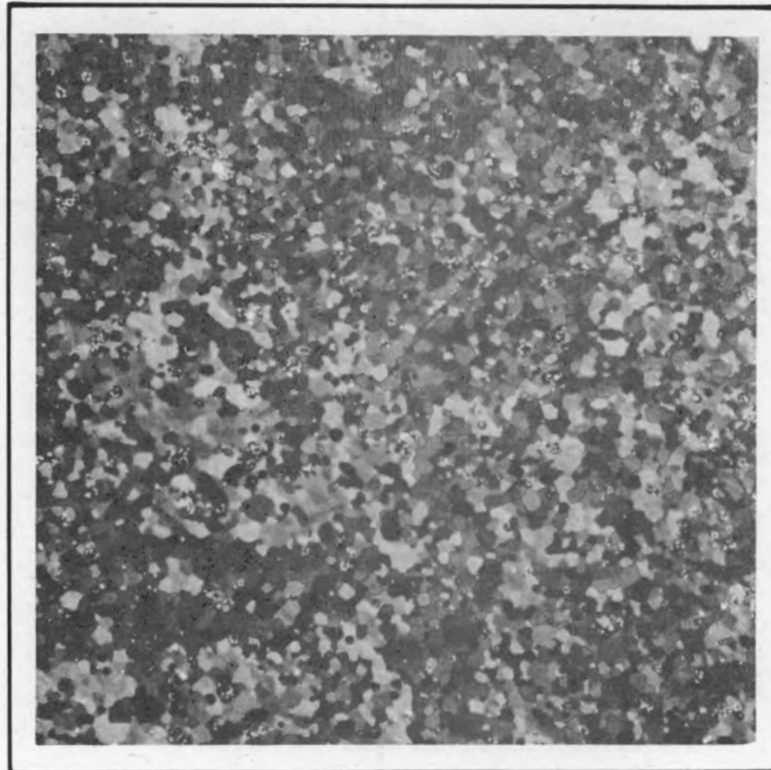


PHOTO NO. Y-1204
M. SPEC.- 785-A
TRANS.

MAG.- 150 X
ETCH- POL. LIGHT

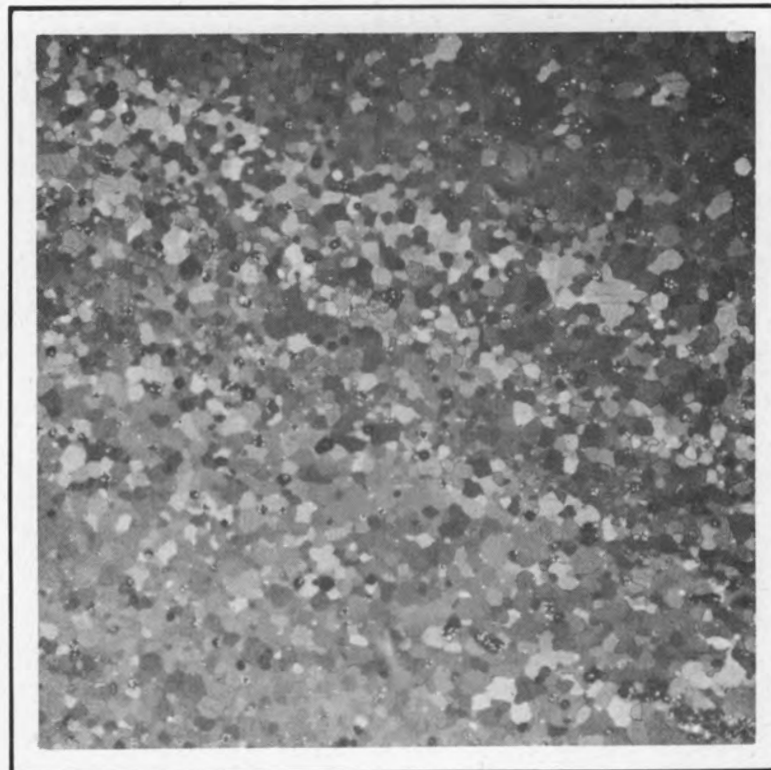


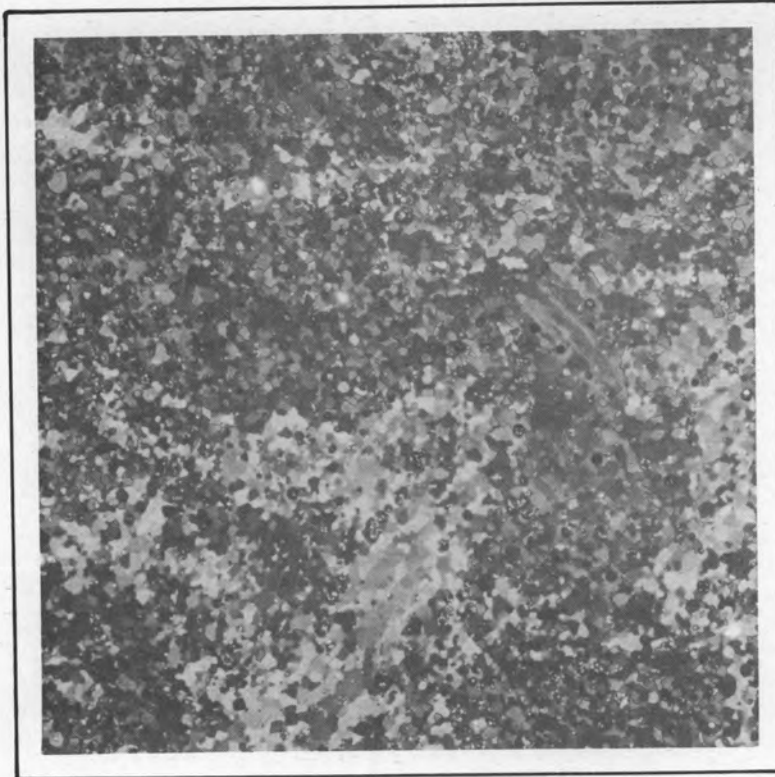
PHOTO NO. Y-1210
M. SPEC.- 785-B
LONG.

PHOTOMICROGRAPH SHOWING THE COMPLETELY RECRYSTALLIZED GRAIN STRUCTURE NEAR THE FRONT END OF A 5/8" DIAMETER α EXTRUDED URANIUM ROD.

FIG. 2.32

NOT CLASSIFIED
Y-3691

PHOTO NO. Y-1209
M.SPEC.- 786-A
TRANS.



MAG.- 150X
ETCH-POL. LIGHT

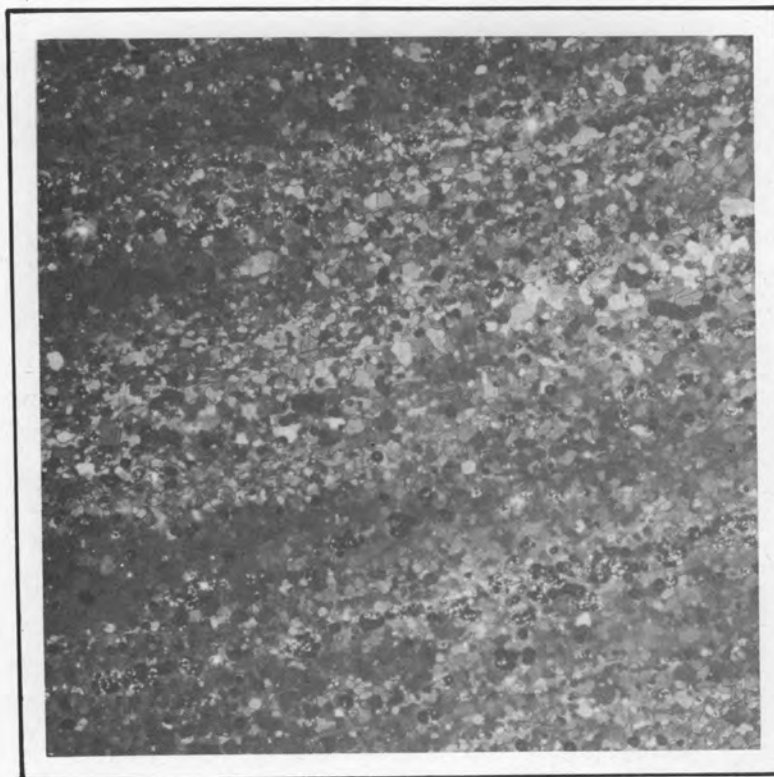
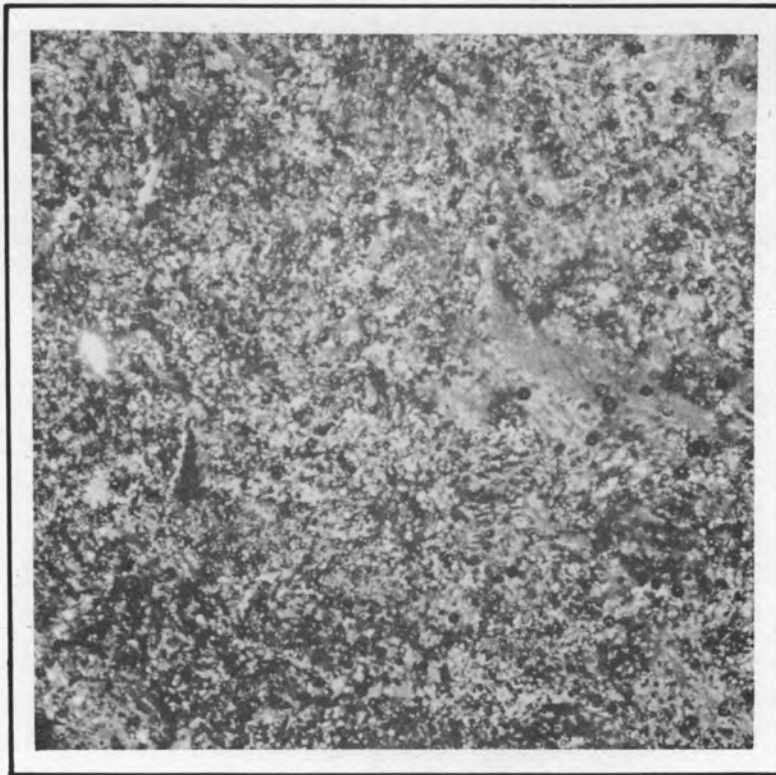


PHOTO NO. Y-1207
M.SPEC.-786-B
LONG.

PHOTOMICROGRAPH SHOWING THE ALMOST COMPLETELY RECRYSTALLIZED GRAIN STRUCTURE IN THE MIDDLE OF THE LENGTH OF A $5/8$ " DIAMETER α EXTRUDED URANIUM ROD.

FIG. 2.33



NOT CLASSIFIED
Y-3692

PHOTO NO. Y-1205
M. SPEC.-787-A
TRANS.

MAG.-150 X
ETCH-POL. LIGHT

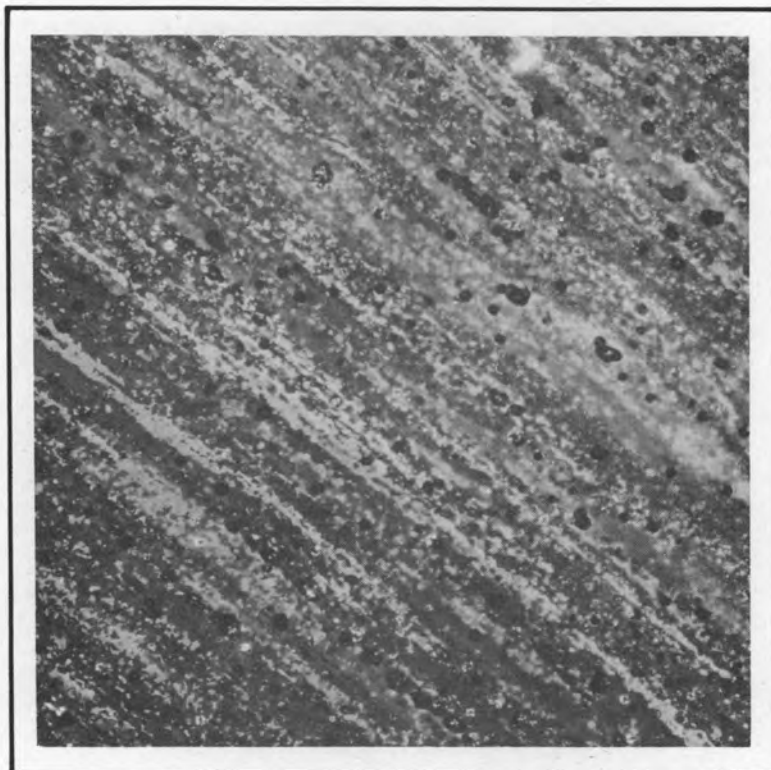


PHOTO NO. Y-1208
M. SPEC.-787-B
LONG

PHOTOMICROGRAPH SHOWING THE PARTIALLY RECRYSTALLIZED GRAIN STRUCTURE NEAR THE BACK END OF A 5/8" DIAMETER α EXTRUDED URANIUM ROD.

FIG. 2.34

The simple experiment of annealing to recrystallize the samples now having a deformed structure and noting the changes in preferred orientation that occur should resolve this uncertainty. This experiment is now underway.

URANIUM BONDING STUDIES

Further tests on silver-mercury bonds between uranium and copper show that superior shear strength is obtained by hot pressing at 5000 psi and 300°C. Values of 6000 psi were obtained with samples hot pressed under these conditions for 2 hr.

A topical report (ORNL-920) has been issued covering details of this work.

Roll Cladding of Uranium With Copper. Additional copper-uranium sandwiches were rolled to obtain more data on the effect of heating on bond strength. Results of heating samples in air and vacuum are given in Table 2.2. Because of the poor results obtained, this work is being discontinued.

TABLE 2.2

Effect of Heating on Strength of Cu-U Bonds

TEMPERATURE (°C)	TIME (hr)	RESULTS OF BEND TESTS
Air Tests		
150	2.5	No separation
	20.5	No separation
	20.5	No separation
300	7	No separation
	7	No separation
	24	Curling of edge
	24	Some separation, 1/8 in. in one case
540	0.5	Some separation; light green
Vacuum Tests		
850	0.5	Complete separation
	0.5	Complete separation
	0.5	Complete separation
300	0.5	Very light separation
	0.5	No separation
	0.5	No separation
600	0.5	Complete separation
	0.5	Very light separation
	0.5	Very light separation

3. ANP PROGRAM

LIQUID-METAL CORROSION TESTING

Research work on the behavior of elementary metals and commercial alloys in liquid-metal media is being continued. Static corrosion tests are being made with considerable emphasis being placed on metallographic examination rather than weight change or solubility measurements to determine the nature and extent of attack. Thermal convection loops containing Na or Pb are being operated by the ANP Experimental Engineering Group at 1350 and 1500°F for varying lengths of time up to 1000 hr. Several loops have been examined. The lack of suitable welded joints appears to be the limiting factor which determines the life of Na-containing loops. The first forced-circulation loop apparatus is being filled with Na for a trial run, also by the Experimental Engineering Group. Some experimental data should be available for the next quarterly report.

Revision of Static Corrosion-testing Technique. The method of static corrosion testing which requires the placing of metal specimens in capsules of iron (for lithium tests) or nickel (for sodium tests) introduces some uncertainty regarding the validity of test results because of a possible interaction between the three components — capsule, specimen, and liquid metal.

A modified "two-component test" in which the container would also serve as the specimen, or is of the same composition as the specimen, is being developed. Methods of purification of the liquid metal and filling techniques are being studied. Several tests made using the two-component technique should indicate the extent to which three-component tests might be in error.

Previous tests have been made for 40- and 400-hr periods; future two-component tests are being planned as 100-hr tests. The effect of time will be established so that the suitability of 100-hr tests can be confirmed.

Static Corrosion-test Data. Sodium. Metals exposed to sodium at 1000°C have shown relatively shallow surface effects; these are summarized in Table 3.1. Some of these effects, such as the carburization of Mo, Ta, Ti, and W, are caused by impurities in the sodium, whereas other effects are probably due to mass transfer, simple solution, or selective leaching of alloy components.

TABLE 3.1

Materials Tested in Sodium at 1000°C

MATERIAL	TIME (hr)	WEIGHT CHANGE (mg)	DEPTH DISSOLVED (in.)	SURFACE		REMARKS
				FILM THICKNESS (in.)	X-RAY IDENTIFICATION*	
Metals						
Co	400	+175	0.0076	None	Co (fcc), Co (hex)	Bright surface, light etched appearance; small voids or particles paralleling the surface to depth of 0.0008 in.
Ni	400	+10	None	None	Ni	Apparently no attack
Mo	400	+75		0.002	Mo ₂ C, Ni	Definite surface film, very hard (2992 Vickers) compared to matrix (206 Vickers); film uniform and adherent; microspectrograph showed Ni penetration to 0.0030 in. (see Fig. 3.1)
Ta	400		None	0.0006	TaC	Surface deposit and diffusion layer; total depth affected, 0.0024 in.; specimens badly blistered and scaled, giving unreliable weight change data
Ti	400	+240	None	0.005	TiC	Heavy uneven surface film or diffusion layer; microspectrographic analysis detected carbon to a depth of 0.0043 in.
W	400	-1050	0.0014	Very thin	WC	Some spotty corrosion at grain boundaries; very thin, brittle film
Alloys						
N155	400	+300	None	0.001	fcc	Matrix appeared heavily carburized with a thin skin of decarburized surface layer; unidentified phase under surface; microspectrograph reported no variations in composition; 0.010 in. increase in thickness
Inconel	400	+160	None	None	fcc	Appeared to have carbides dispersed throughout the matrix except at the surface. Decarburization to a depth of 0.0012 in.; no intergranular attack (Fig. 3.2)
Inconel X	400	+100	None	None	fcc	Intergranular attack to 0.0016 in.; decarburization about 0.0006 in.; precipitate in grain boundaries and peppered within the grains to about 0.0492 in.; slight increase in thickness (Fig. 3.2)
304 SS (0.006% C)	40	-200	None	None	Not reported	Heavy grain boundary precipitate; some phase in crystallographic planes in needles; heavy corrosion, leaving a very rough surface, to a maximum depth of 0.0028 in.
310 SS	40	-60	None	None	fcc, Cr ₂ O ₃	Heavy carbide precipitate in grain boundaries below the decarburized layer; some corrosion voids in decarburized layer, which was 0.002 in thick
347 SS	40	-60	0.0025	None	fcc, Cr ₂ O ₃	0.0008 in. decarburization and 0.0005 in. intergranular penetration
430 SS	40	-165	No data	None	fcc, Cr ₂ O ₃	Slight intergranular attack to 0.0025 in.; some decarburization to 0.001 in.; nonuniform sigma-like precipitate to a depth of 0.025 in.
446 SS (0.006% C)	40	-50	0.0013	None	No data	Angular sigma-like constituent formed within the grains and also appeared as a precipitate in the grain boundaries

*fcc = face-centered cubic, hex = hexagonal.

The behavior of Mo, shown in Fig. 3.1, indicates mass transfer of Ni from the capsule to the specimen. Effects of temperature alone, i.e., grain growth and uniform precipitation of equilibrium phases throughout the specimen, have also been observed but are not emphasized.

All the metals and alloys reported in Table 3.1 have shown satisfactory stability in the presence of liquid sodium at 1000°C except tungsten, which appears to be slightly attacked in sodium, and low-carbon type 304 stainless steel, which appears to be susceptible to intergranular attack. A comparison of nickel, Inconel, and Inconel X indicates that the Inconel is definitely superior to the Inconel X as far as corrosion is concerned, while nickel is superior to both, as can be observed in Fig. 3.2.

Lithium. In addition to the tests run at 1000°C, several tests have been made on metals in lithium at 700 and 850°C. These data are not yet available for presentation.

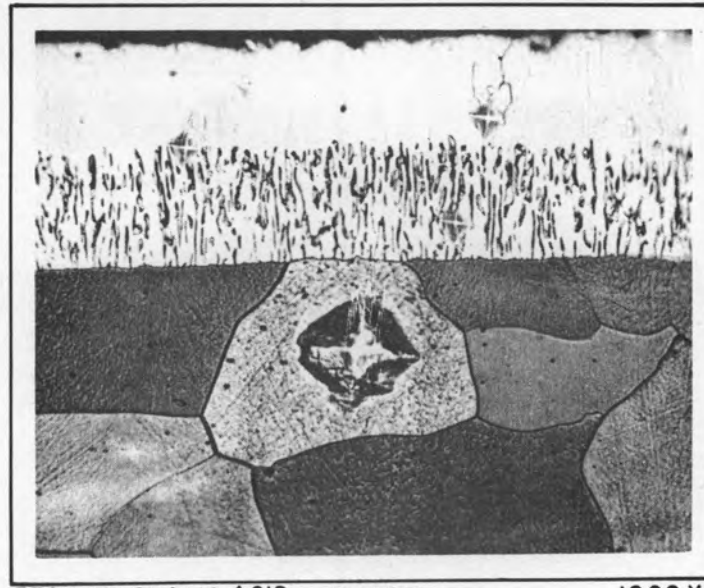
Lead. Metal samples placed in lead at 1000°C have shown a wide variation in behavior (see Table 3.2); thorium and uranium have demonstrated appreciable solubility, whereas Zr, Cb, Mo, and Ta have shown no evidence of solution.

Austenitic steels bordering on the ferritic region have shown evidence of surface and near-surface grain boundary diffusion. These regions transform to ferrite, as is shown in Fig. 3.3.

The presence of light gray particles in the surface layers of types 410 and 430 ferritic steels suggests that lead diffuses into the metal surface, as shown in Fig. 3.4. Such particles are difficult to retain during polishing and are probably the cause of the sub-surface voids which are reported in the ferritic stainless steels, e.g., type 446, shown in Fig. 3.4. Some gray particles have been retained.

2 Atomic % Uranium — 98 Atomic % Bismuth. A number of metals, tabulated in Table 3.3, in contact with bismuth containing 2 atomic % uranium at 1000°C have shown widely varying behavior. Titanium, zirconium, and Inconel have been severely attacked, whereas columbium, molybdenum, tantalum, and tungsten are quite stable.

Type 316 stainless steel, although susceptible to liquid-metal attack along surface grain boundaries (Fig. 3.5), is quite superior to Inconel.



NICKEL
MOLYBDENUM
ALLOY
D.P.H. 2990

0.001
in.

0.005
cm.

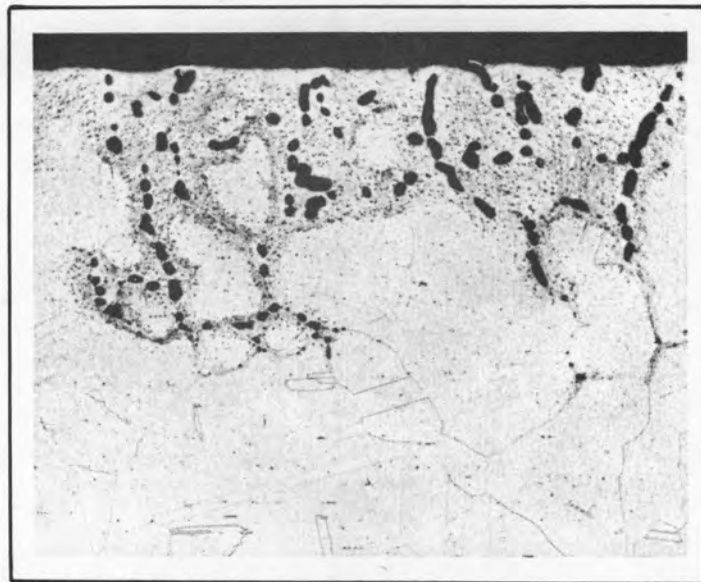
MOLYBDENUM
D.P.H. 250

ETCH: 5% OXALIC ACID Y-2772 1000 X

DIAMOND PYRAMID HARDNESS IMPRESSIONS IN TRANSFER LAYER AND BASE METAL.

MASS TRANSFER FROM NICKEL CAPSULE TO MOLYBDENUM SPECIMEN IN LIQUID SODIUM.

400 HOURS AT 1000°C
FIG. 3.1



0.010
in.

0.050
cm.

ETCH: AQUA REGIA Y-2906 100X

AUSTENITE-FERRITE TRANSFORMATION AT SURFACE AND GRAIN BOUNDARY
IN AUSTENITIC STAINLESS STEEL.

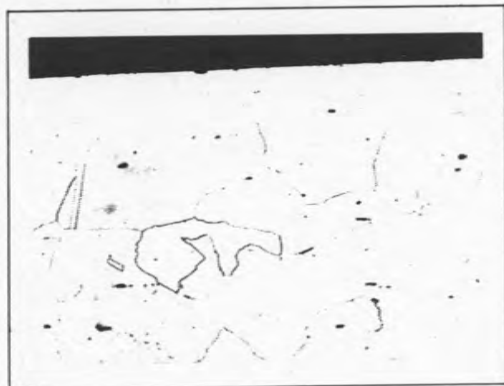
TYPE 304 LOW CARBON STAINLESS STEEL EXPOSED TO LEAD.

400 HOURS AT 1000°C
FIG. 3.3

BEFORE EXPOSURE

NOT CLASSIFIED
Y-3875

NICKEL

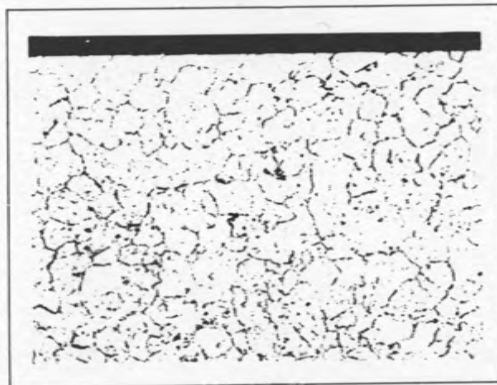


Y3859

ETCH: $H_2SO_4 - H_2O$

250X

INCONEL



Y3086

ETCH: OXALIC ACID

250X

INCONEL-X

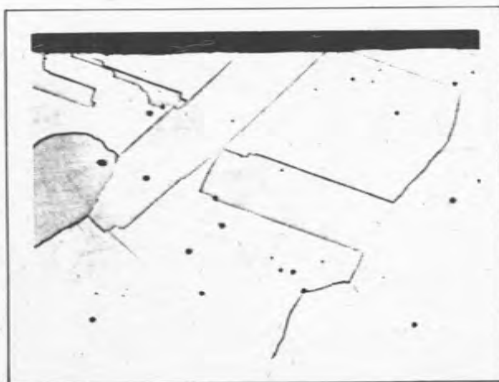


Y3085

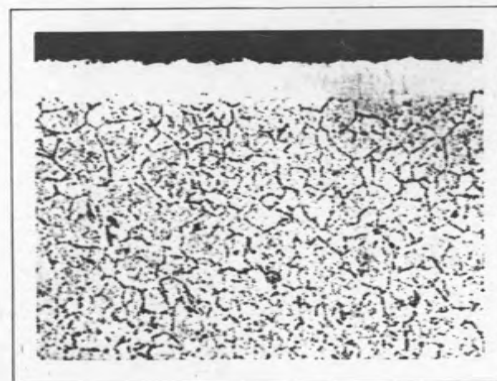
ETCH: OXALIC ACID

250X

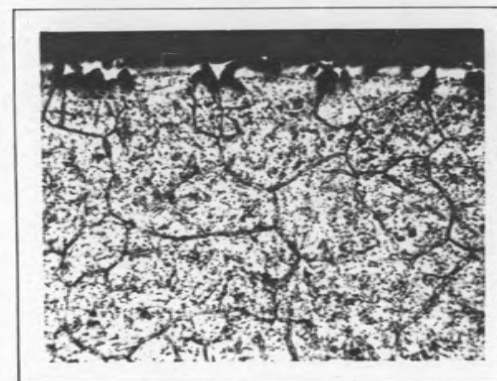
42



Y2742



Y2749

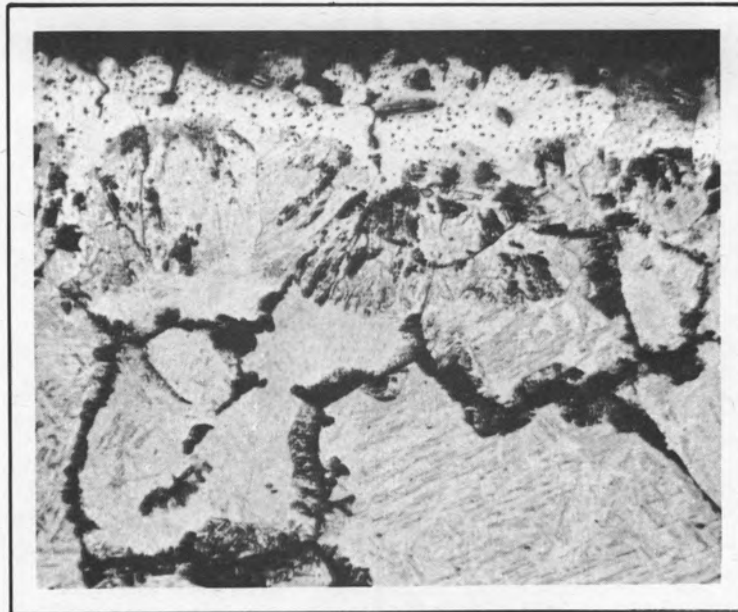


Y2760

AFTER 400 HOURS EXPOSURE

CORROSION SPECIMENS EXPOSED TO SODIUM
1000°C

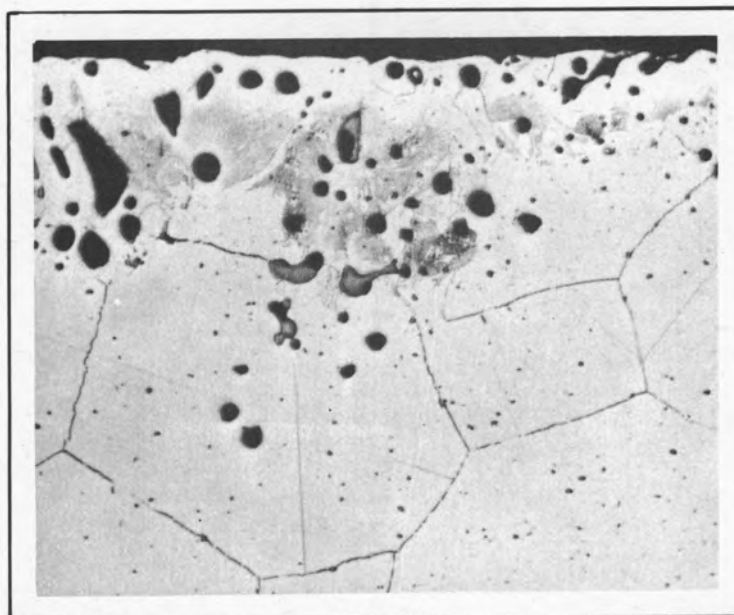
FIG. 3.2



0.004
in.
0.020
cm.

ETCH:PICRAL, HCL. Y-2905 250 X

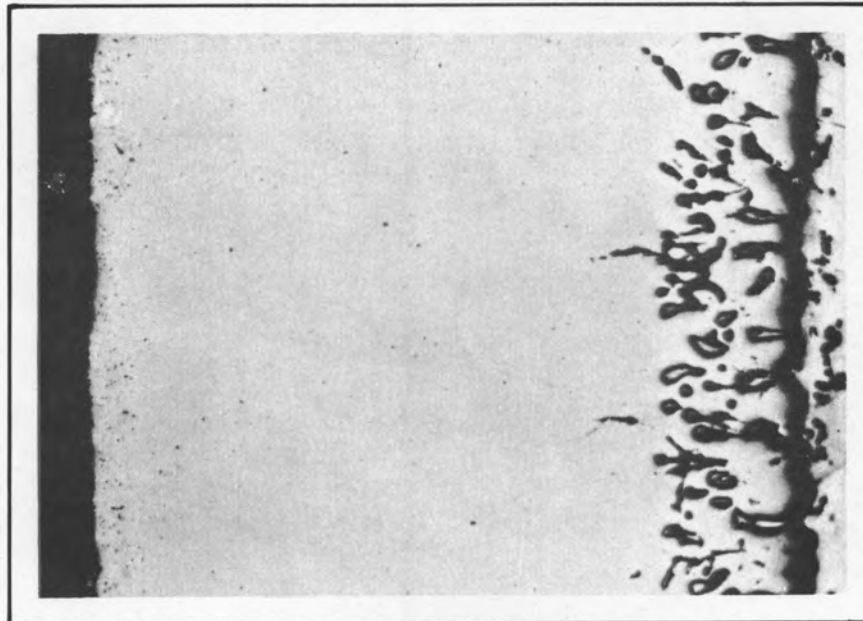
TYPE 410 EXTRA LOW CARBON, SHOWING LIGHT GREY PRECIPITATION,
AND SOME GRAIN BOUNDARY PENETRATION TO DEPTH OF .003 IN.



0.005
in.
0.025
cm.

ETCH:PICRAL Y-2875 200 X

TYPE 446 VERY LOW CARBON SHOWING LAMELLAR STRUCTURE AND
GLOBULAR VOIDS, SOME PARTIALLY FILLED WITH GREY SUBSTANCE
STAINLESS STEELS EXPOSED TO LEAD
400 HOURS AT 1000°C

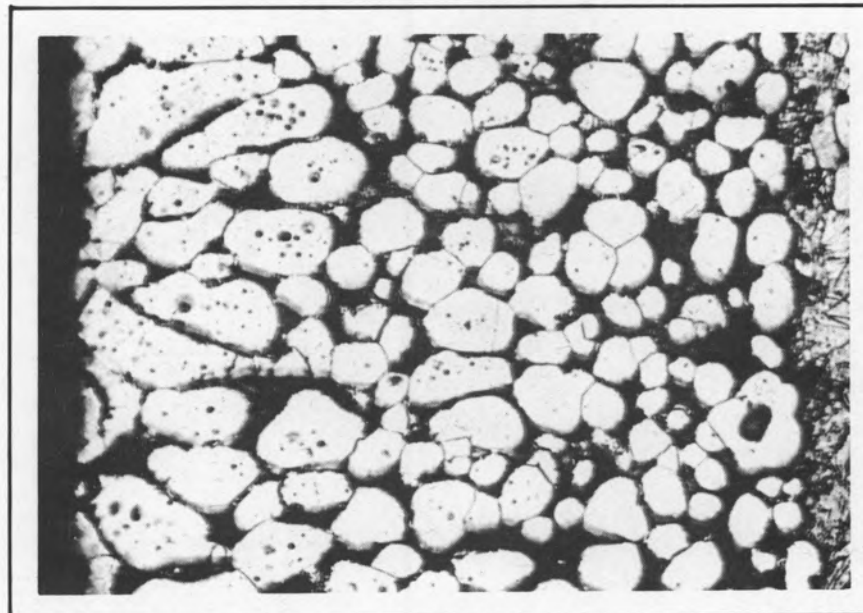


ETCH: NONE Y-3081 175X

316 STAINLESS STEEL
PARTIAL INTERGRANULAR PENETRATION BY
ALLOY
TUBE WALL

0.006
in.
0.029
cm.

Bi-U
ALLOY



ETCH: OXALIC ACID,
AQUA REGIA Y-3124 175X

INCONEL
COMPLETE INTERGRANULAR PENETRATION BY
ALLOY

**CORROSION TUBE SPECIMENS EXPOSED TO
Bi-U ALLOY
40 HOURS AT 1000°C**

FIG. 3.5

TABLE 3.2

Materials Tested in Lead at 1000°C

MATERIAL	TIME (hr)	WEIGHT* CHANGE (mg)	DEPTH DISSOLVED (in.)	X-RAY IDENTIFICATION** OF SURFACE	REMARKS
Metals					
Zr	40	+70	No data	Pb, PbO ₂ , ZrO ₂	Very thin surface film; no other attack detected
Cb	40	+140	No data	Pb, PbO, PbO ₂ , Cb	Continuous, uniform, spongy-appearing film, softer than base metal
Mo	40	+250	No data	bcc	Surface deposit with perpendicular fractures; no corrosion
Ta	40	+150	No data	Ta, TaC, PbO, PbO ₂	Bright film harder than base metal appeared to have been deposited
W	40	+35	No data	W, WC, Pb, PbO	No film or attack observed; W not detected in bath
Th	40	Samples dissolved			
U	40	Samples dissolved			
Alloys					
45 304 SS (0.04% C)	40	-175	0.008	bcc	Some intergranular attack to 0.0032 in.; slight phase change along attacked grain boundaries and surface
	400	+190	None	bcc	Transformation along attacked grain boundaries to 0.025 in.; precipitation in alpha and gamma regions; intergranular penetration to 0.025 in.; no decarburization
304 SS (0.006% C)	40	-90	0.0008	bcc, Cr ₂ O ₃	Heavy intergranular attack with phase transformation along attacked grain boundaries to depth of 0.0106 in., (Fig. 3.3)
310 SS	40	+75	No data	fcc, Pb, PbO	Intergranular attack to 0.015 in. with some decarburization to 0.015 in.; a fine precipitate scattered throughout specimen, primarily at grain boundaries
316 SS	40	+5	None	bcc, Pb, PbO	Thin transformation zone, 0.0005 in., along exposed surface and also in grain boundaries near surface; intergranular type attack to 0.008 in., voids in clear white precipitate at grain boundaries
347 SS	40	-20	None	bcc, Pb, PbO	Intergranular type attack, 0.008 in.; phase transformation in attacked region
405 SS	40	-165	None	bcc	Very slight attack
	400	+135	0.0051	bcc, fcc, Pb	Intergranular type attack; surface rough; corrosion voids to depth of 0.005 in.; some decarburization, light gray precipitate to 0.006 in.

TABLE 3.2 (Cont' d)

MATERIAL	TIME (hr)	WEIGHT* CHANGE (mg)	DEPTH DISSOLVED (in.)	X-RAY IDENTIFICATION ** OF SURFACE	REMARKS
410 SS (ELC)***	40	+30	None	bcc, Cr ₂ O ₃	Intergranular attack to 0.0019 in.; blue-gray compound formed at surface. (Fig. 3.4)
	400	+300	0.0076	bcc, PbO	Possible film or mass transfer layer to 0.002 in. that is laced with voids; depth of intergranular penetration 0.004 in.; light gray precipitate in decarburized area (0.006-in.-deep area)
430 SS	40	-40	None	bcc	Intergranular corrosion attack to 0.0012 in.
	400	+100	0.0076	bcc	Intergranular corrosion voids to 0.004 in.; some light gray precipitate to 0.006 in.; some decarburization to 0.006 in.
430 SS (ELC)	40	-75	0.0025	bcc, Fe-Cr solid solution	Blue-gray compound on surface and in grain boundaries near surface; clear precipitate in matrix
446 SS	40	-60	0.0003	No data	Globular voids near exposed surface to 0.0039 in.; heavy decarburization to 0.0063 in.; large sigma-like precipitate in center of specimen
446 SS (ELC)	40	-75	0.0026	No data	Irregular attack; large voids concentrated along surface; some precipitate, large grain size
446 SS (0.006% C)	40	-60	0.006	bcc	Decarburized area adjacent to edge laced with voids to 0.0024 in.; some voids contained gray precipitate

* Weight change data on samples tested in lead are not sufficiently accurate to be significant owing to lead adhering to the specimen.

** bcc = body-centered cubic; fcc = face-centered cubic.

*** ELC = extra low carbon (<0.05% C).

TABLE 3.3

Materials Tested in Bismuth-Uranium Alloy at 1000°C

MATERIAL	TIME (hr)	X-RAY IDENTIFICATION OF SURFACE	REMARKS
Beryllium	4	Bi ₂ O ₃ *	Uneven surface, indicating some corrosion attack; no diffusion apparent
Titanium	4	Sample dissolved in bath	
Armco iron	4	FeO, Bi ₂ O ₃	Uneven surface with dark noncontinuous film, brittle; film less than 0.0005 in. thick
Zirconium	4	Zr, ZrO ₂	Sample nearly dissolved; no metallographic data
Columbium	100	UO ₂ , Cb	Very thin surface deposit (nonadherent); no other corrosion
Molybdenum	100	Mo, UO ₂ , Bi ₂ O ₃ *	Faint suggestion of surface film and no change in structure; some grain growth; no other visible corrosion
Tantalum	100	Ta, UO ₂ , Bi ₂ O ₃ *	Very thin films on surface
Tungsten	4	W, UO ₂ , Bi ₂ O ₃ *	Very uniform surface; no visible film or corrosion
Inconel	40	No data	Tube sample tested, complete leakage by penetration of BiU along grain boundaries throughout sample; very porous and brittle (Fig. 3.5)
	100	No data	BeO crucible leaked during test; penetration through the ¼-in.-thick sample; very brittle and porous
316 SS	40	No data	Intergranular penetration to 0.009 in. (Fig. 3.6)
	100	No data	BeO crucible leaked during test; sample still had extremely heavy intergranular penetration to 0.025 in.

* X-ray lines were also seen corresponding to those of original 2 atomic % U—98 atomic % Bi alloy.

Dynamic Corrosion Testing. During the past quarter the ANP Experimental Engineering Group has operated various thermal convection loops and turned them over to the ORNL Metallurgy Division for examination. The loops are listed in Table 3.4.

TABLE 3.4

LOOP NO.	LOOP MATERIAL	HOT ZONE TEMP. (°F)	LENGTH OF OPERATION (hr)	REMARKS
Sodium Loops				
1	316 SS	1350	1100	Scheduled termination
2	316 SS	1350	979	Leak in top plug
3	316 SS	1500	1000	Scheduled termination
4	316 SS	1500	625	Hot leg failure
5	304 SS	1500	349	Weld failure
6	L-605*	1500	1000	Scheduled termination
7	347 SS	1500	1000	Scheduled termination
8	SAE 1010 steel	1200	593	Hot leg failure
9	Nickel	1500	0	Weld failure
10	SAE 1010 steel	1200	25	Weld failure
11	Nickel	1500	13	Weld failure
13	Nickel	1500	223	Weld failure
14	347 SS	1350	1000	Scheduled termination
15	347 SS	1350	1000	Scheduled termination
16	304 SS	1350	1000	Scheduled termination
17	304 SS	1350	1000	Scheduled termination
Lead Loops				
26	316 SS	1500	138	Internal plugging
27	316 SS	1500	0	Internal plugging
28	446 SS	1500	62	Internal plugging

* L-605 is a cobalt-base wrought alloy, also known as "Haynes Alloy No. 25."

The loops listed in Table 3.5 are either in operation or in the process of metallographic examination.

TABLE 3.5

LOOP NO.	LOOP MATERIAL	HOT ZONE TEMP. (°F)	LIQUID METAL	LENGTH OF OPERATION (hr)	REMARKS
12	Nickel	1500	Sodium	1000	Operation completed; loop being cleaned
29	Inconel	1350	Sodium		In operation
30	310 SS	1350	Sodium		In operation
33	321 SS	1500	Sodium	754	Hot zone failure
34	321 SS	1500	Sodium	457	Loop badly distorted
37	V-36*	1500	Sodium		In operation
39	V-36*	1500	Lead		In operation
36	L-605*	1500	Lead		In operation
	V-36*	1500	Lithium		
	L-605*	1500	Lithium		
19	SAE 1010 steel	1100	Lead		In operation
21	SAE 1010 steel	1100	Lead		In operation
35	SAE 1010 steel	1400	Lead		In operation

*V-36 and L-605 are cobalt-base wrought high-temperature alloys.

The loops given in Table 3.6 are being constructed.

TABLE 3.6

NO. OF. LOOPS	LOOP MATERIAL	FABRICATOR	PROBABLE LIQUID METAL	PROBABLE OPERATING TEMP. (°F)
2	304 SS	ORNL Shops	Lead	1500
2	309 SS	ORNL Shops	Lead	1500 (Cb stabilized)
2	405 SS	ORNL Shops	Lead	1500
2	405 SS	ORNL Shops	Lithium	1500
1	405 SS	ORNL Shops	Sodium	1500
2	410 SS	ORNL Shops	Lithium	1500
2	410 SS	ORNL Shops	Lead	1500
1	410 SS	ORNL Shops	Sodium	1500
1	SAE 1010 steel	ORNL Shops	Lead	1400
2	Inconel	Philadelphia*		
2	446 SS	Philadelphia		
2	310 SS	Philadelphia		
3	316 SS (ELC)	Philadelphia		
5	Stainless steel loops internally coated with SAE 1010 steel	Philadelphia		
2	Nickel	Y-12 Shops	Sodium	1500
2	347 SS	Y-12 Shops		

* Philadelphia Pipe Bending Co.

A lithium-loop-filling device, in which the lithium is aged and filtered, has been fabricated and set up at Y-12. Lithium loops are scheduled to be in operation by the middle of February. A similar device to be used for lead is being fabricated and should be ready during March. Temporarily loops are being filled with lead by members of the ORNL Metallurgy Division.

Thermal Convection Loops. The thermal convection loops were filled with aged and filtered sodium or drossed lead. Sodium samples were taken during filling for oxygen analysis. The hot legs of the convection loops were electrically heated. During operation the cups and cold leg were allowed to air-cool with no external heating or cooling. With this type of operation temperature gradients from 150 to 300°F were obtained. The loops were operated for 1000 hr or until failure occurred. At the completion of the test, samples of sodium and lead were taken for oxygen and metal constituent analysis. Metallographic examination of loop segments constituted the primary method of evaluating various metals for corrosion resistance to different liquid media.

A preliminary report on loops 1 through 11, 13 through 17, and 26 through 28 follows: Except for loops No. 6 and 28, which were fabricated at the Philadelphia Pipe Bending Company, all these thermal convection loops were fabricated in the ORNL Central Shops. These loops were fabricated by metal arc welding. All the welds showed poor penetration of the weld metal, and a few of the welds showed internal porosity and slag inclusions in the weld metal.

After fabrication, the loops were acid pickled in an effort to remove scale. In several cases loops that were pressure tested before pickling failed in pressure testing after pickling. Unfortunately it is nearly impossible to separate the pickling attack from that which occurred during the operation of the loop with liquid metal. In some of the unstabilized stainless steels used with sodium, intergranular corrosion frequently occurred in the metal near the welds. In either event, carbide precipitation during welding undoubtedly made the material susceptible to intergranular attack.

At the present time the oxygen and spectrographic analyses of the sodium and lead are incomplete and the results of metallographic examination of the loops are only partially available. Hence, the following should be considered as tentative data.

Oxygen analyses of the sodium from two stainless steel loops and one nickel loop have indicated that the oxygen content of the sodium decreased during operation. Spectrographic examination of the sodium taken from two nickel loops (11 and 13) indicated a nickel content of several thousand parts per million.

With the exception of the low-carbon steel loops there was no indication of any appreciable attack on the loops by the sodium. Film formation and mass transfer effects were not observed in any of the sodium-containing loops.

All the lead loops were plugged internally during operation. These plugs consisted of a spongy mass of dendritic crystals, and chemical and spectrographic analyses indicate them to be primarily iron and chromium with possibly small amounts of nickel. The plugs formed in the cold zones of the loop during operation. The mass transfer effect is probably associated with the temperature gradient in the loop.

There was a small amount of intergranular attack in some of the specimens near welds. The type 347 stainless steel loops (7, 14, and 15) showed no evidence of either sigma formation or intergranular attack. The type 304 stainless steel loops showed no sigma formation but there was some intergranular attack adjacent to the welds.

A metallographic examination of the L-605 and nickel loops (6 and 13) showed no perceptible corrosion effects. The metallographic examination of the iron loops is incomplete.

Forced Circulation Loop. The ANP Experimental Engineering Group has constructed a forced convection loop of type 316 stainless steel. At the present time the loop will be operated with sodium to test the electromagnetic pump and other component parts. The loop is heated with Nichrome heating elements and cooled by a built-in heat exchanger and forced circulation of air over the cooling section. Test sections are located in the hot and cold zones, and the loop has been designed to give a maximum velocity of 50 ft/sec through the test section. The ANP Engineering Group has designed and is fabricating the following devices to be used in the test sections: self-welding apparatus, stress-corrosion apparatus, seal and bearing test apparatus, and internal pressure gauges.

Two more forced-circulation loops of type 347 stainless steel are being fabricated in the Y-12 Shops, and 10 loops are in the planning stage. Initially, types 304, 316, and 347 stainless steel and Inconel will be tested in the sodium forced-circulation loop:

POWDER METALLURGY — FUEL ELEMENT FABRICATION

Actual work on members suitable for incorporation into a solid fuel element for a high-temperature reactor has begun. Present efforts are toward developing a plate that could be either used as made or could be fabricated into a tube. This plate is to have the following characteristics:

1. A layer of UO_2 must be held in a metallic matrix. For the present work iron, stainless steel, and molybdenum are being investigated.
2. The fuel layer must be clad on one side or both sides.
3. The fuel layer is to be approximately 0.005 in. and the cladding 0.010 in.

The following three methods of fabrication for such a plate have shown promise and are now being actively pursued:

1. Filling the holes in a perforated metal plate with UO_2 and cladding.
2. Sintering a loose powder to a plate.
3. Using a powder compact and cladding with a technique similar to that used in producing MTR plates.

Sintering a Loose Powder. Several processes in industry achieve a bond by simply sintering a loose powder. An attempt has been made to produce a fuel plate by such a procedure. The facilities of the Micro Metallic Corporation of Glen Cove, N. Y., were used for this work. The process used was based upon confidential techniques developed by this company for the production of metallic filters. In general, the method involved sintering at very high temperatures in a purified, highly reducing atmosphere. Two classes of plates were made, one class with stainless steel powders bonded to stainless steel plates and the other with a mixture of UO_2 and stainless steel powder bonded

to the plate. The purpose of the first class was to determine the feasibility of bonding by this method and possibly to fabricate a porous plate that could later be impregnated.

When only the stainless steel powders were used, a poor metallurgical bond was obtained. This bond is enough to bind the layers to the plate and to resist some flexing, but is not sufficiently good for heat transfer. The amount of bonding was greatly increased by working the plate and resintering. In some cases it was not possible to locate the original interface. Finer stainless steel particles gave a better bonded, but more dense, layer. When type 410 stainless steel was used as the base plate, a zone of martensite was found well up into the powder layer.

If 20% (by volume) UO_2 is added to the stainless steel powder, the bonding is partially inhibited. In some cases not even a mechanical bond was obtained. Figures 3.6 to 3.9 are from a series of this type with 20% UO_2 added to type 316 stainless steel powder and sintered onto a 316 plate. Figure 3.6 is in the as-sintered condition and shows a very poor bond both to the base plate and in the powder layer itself. Nearly all the powder has fallen out during polishing. Pressing (100 tsi) and resintering (Fig. 3.7) increase the bond enough to bind the material together and to the plate, but not enough for adequate heat transfer. The UO_2 is well distributed, and a network of stainless steel does exist. Figures 3.8 and 3.9 show the effects of rolling and resintering. The amount of bond has been increased, but the UO_2 is now found in stringers parallel to the plate, which is undesirable.

A second plate was prepared similar to the one just discussed except that a cladding on both sides was desired. No provision could be made for ensuring contact of the top cladding plate, so it is not surprising that very little bonding took place at this interface. The bonding at the bottom interface was much better than the one previously discussed but is still not adequate. Pressing and resintering this compact produced a good bond at the bottom and a fair one at the top (Fig. 3.10). When this plate was cold rolled and resintered, the bond was improved, but again the UO_2 stringers were found.

A plate similar to the first one discussed above but with a type 410 base plate was made. The results on this plate were very similar to those discussed above except that martensite formation was evident.

~~SECRET~~

Y-3184

Mounting Bar

Remains of powder layer

Interface
316 Cladding



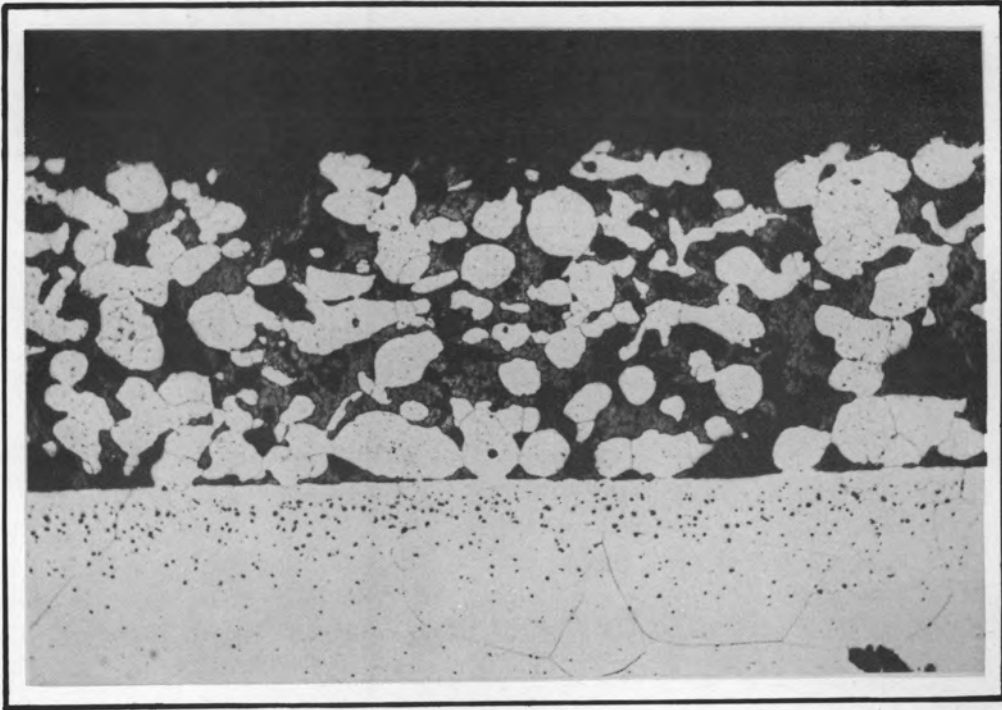
0.021 in.

FIG. 3.6
200x

Y-3135

Clad 316-UO₂(20%) powder compact. As sintered.

316-UO₂(20%)
powder layer



0.012 in.

FIG. 3.7
200x

Y-3136

Clad 316-UO₂(20%) powder compact. Sintered, pressed and resintered.

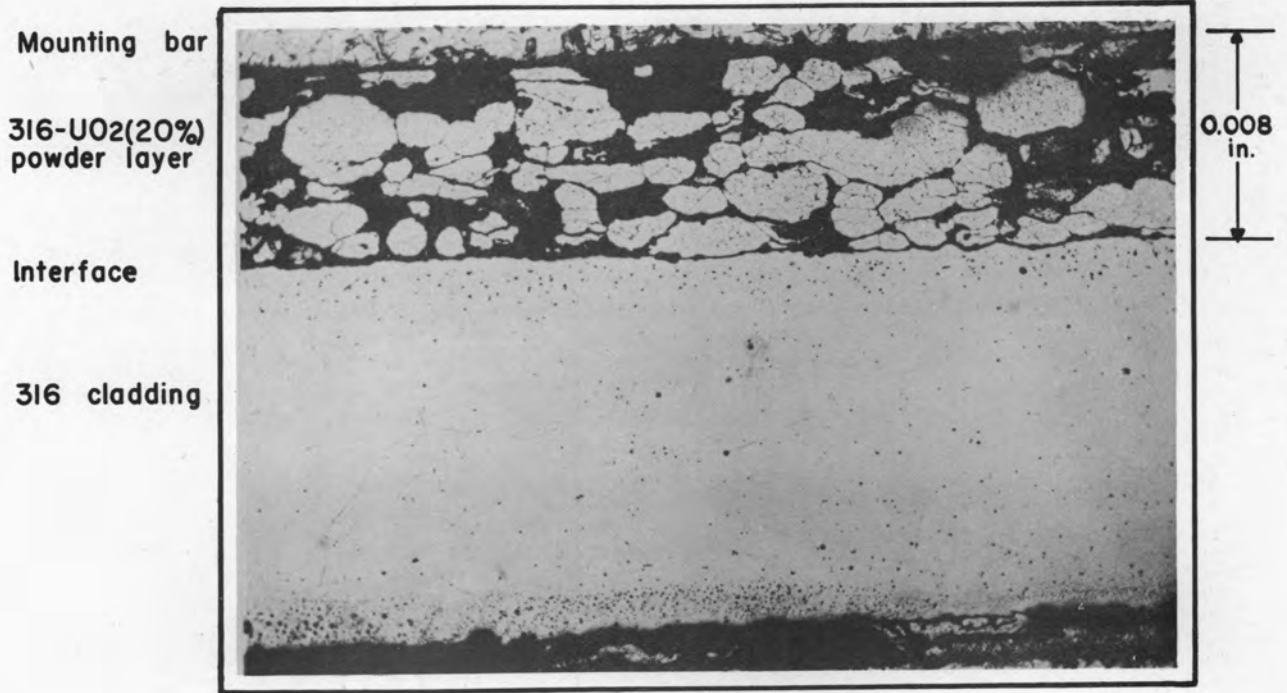


FIG. 3.8
200x

Y-3138

Bond of 316-UO₂(20%) compact to 316 plate sintered and rolled 50%.

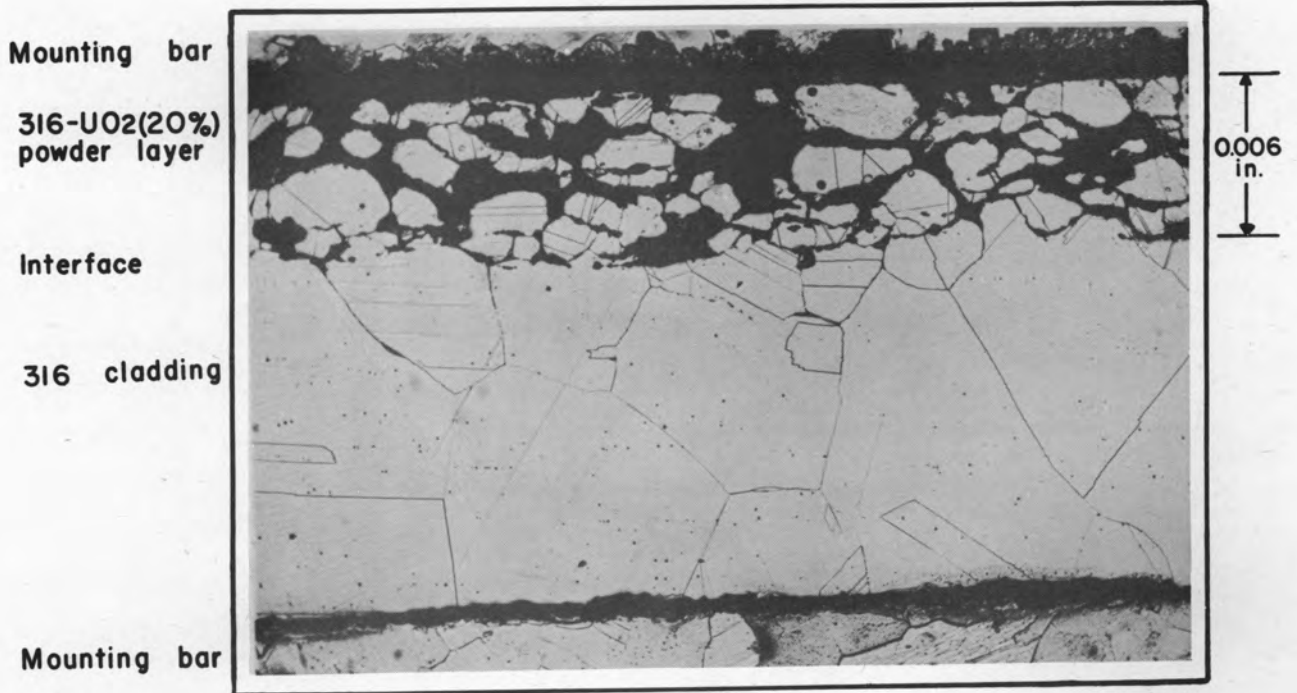


FIG. 3.9
200x

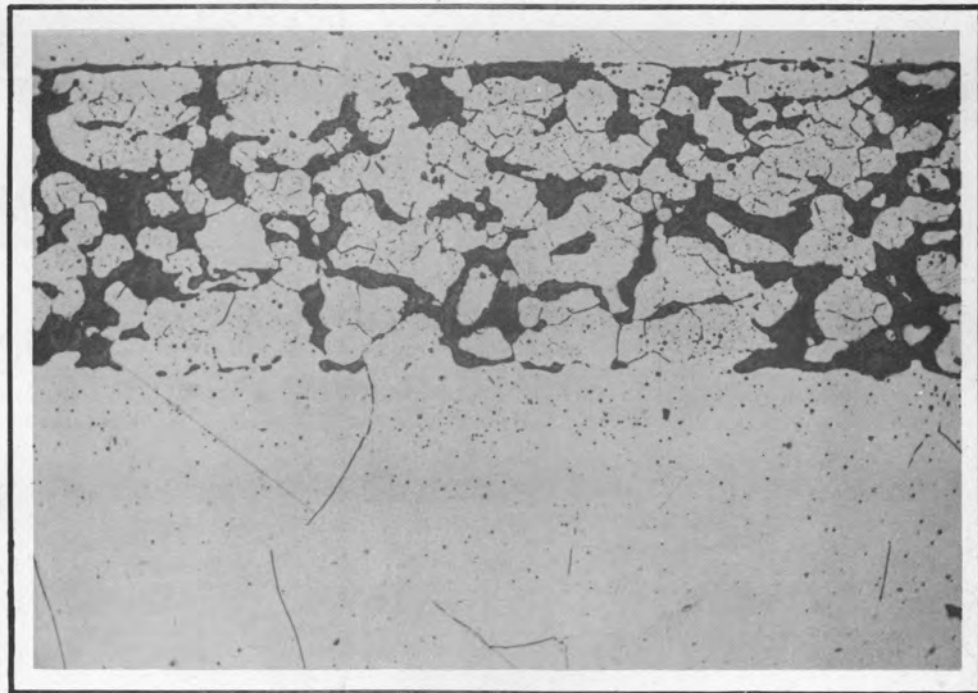
Y-3139

Bond of 316-UO₂(20%) compact to 316 plate sintered, rolled 50% and resintered.

316 Cladding

316-UO₂(20%)
powder layer

316 Cladding



0.012
in.

FIG. 3.10
200x

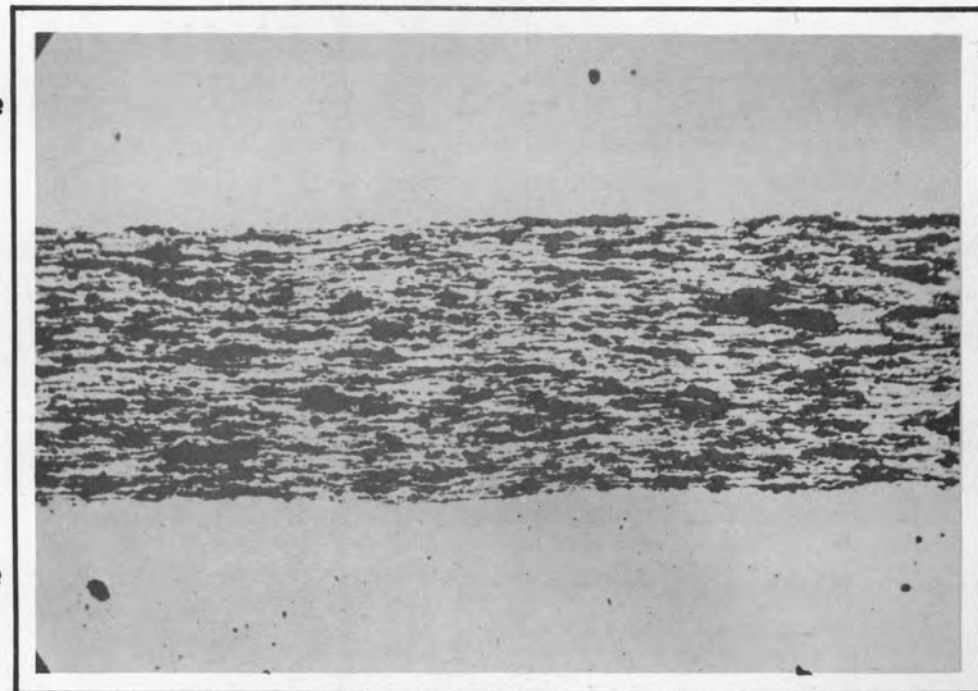
Y-3137

Double clad 316-UO₂(20%) loose compact. Sintered,
pressed and resintered.

316 plate

302-UO₂(30%)
pressed compact

316 plate



0.010
in.

FIG. 3.11
175x

Y-3144

Double clad 302-UO₂(30%) pressed compact. Hot
rolled 90%.

MTR Type Fuel Plate. If a plate or tube with a cladding on both sides is desired, a technique similar to that used for making MTR fuel plates might possibly be adapted. To investigate this possibility disks 1 in. in diameter and 0.140 in. thick were fabricated. These disks were of both 30 and 50% UO_2 and were prepared with both iron and stainless steel matrices. The stainless steel used was 100-mesh electrolytic powder while the iron was 10- μ carbonyl powder. The disks were framed and covered with type 316 plate.

Since a suitable protective atmosphere was not available, the sandwiches were canned in flattened stainless steel tubes and the tubes were evacuated to 50 μ Hg and sealed. With the iron compacts 0.035-in. tubes were welded closed with a hand torch. During rolling at 1330°C every can failed. The stainless steel compacts were then canned in 0.065-in. tubes and sealed with a heliarc weld. This procedure eliminated the can failures.

Figures 3.12 to 3.14 are representative of the various plates containing an iron- UO_2 fuel layer. The plate in Fig. 3.12 contains 30% UO_2 and has been reduced 54%; it is typical of plates with small reductions. One interface is bonded, but at the other a void is found. It appears that the sides of this void have partially bonded and then torn away. Figure 3.13 is from the same type of plate reduced 80%. In this sample both interfaces are well bonded, and the UO_2 is quite evenly distributed in a metallic matrix. A core containing 50% UO_2 which has been reduced 78% is shown in Fig. 3.14. Even with this high UO_2 concentration, good bonds and a continuous metallic network are found. The third phase present at the interface of these compacts appears to be a diffusion zone between the iron and stainless steel.

In all these samples the can was completely bonded to the cover plate, making stripping impossible. Another major problem will be the maintaining of dimensional tolerances. An unexplained variation in the thickness of the rolled powder compact occurred in all these tests.

Metallographic examination of the plates containing the type 302 stainless steel matrix is not completed; however, Fig. 3.11 is presented for comparative purposes. This plate contains 30% UO_2 and has been reduced 90%. Both interfaces show good bonding, but the UO_2 is again present as undesirable stringers. Further work with a finer stainless steel powder is planned.

Y-3187

Fe-UO₂(30%)
Pressed Compact

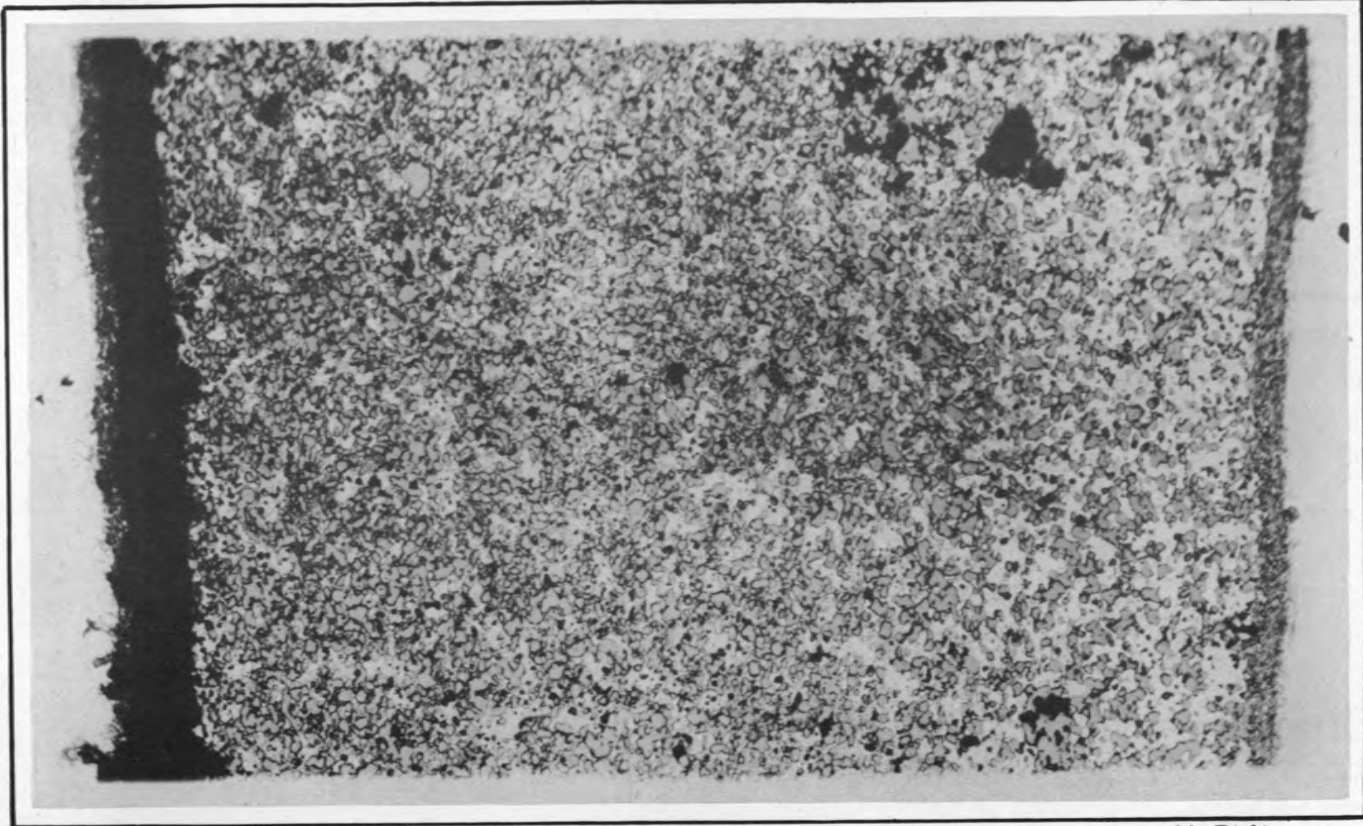
Void

Interface

316 Cladding

316 Cladding

0.010
in.



58

FIG. 3.12
175 x

Y-3141

Double Clad Fe-UO₂(30%) Pressed Compact. Hot Rolled 54%.

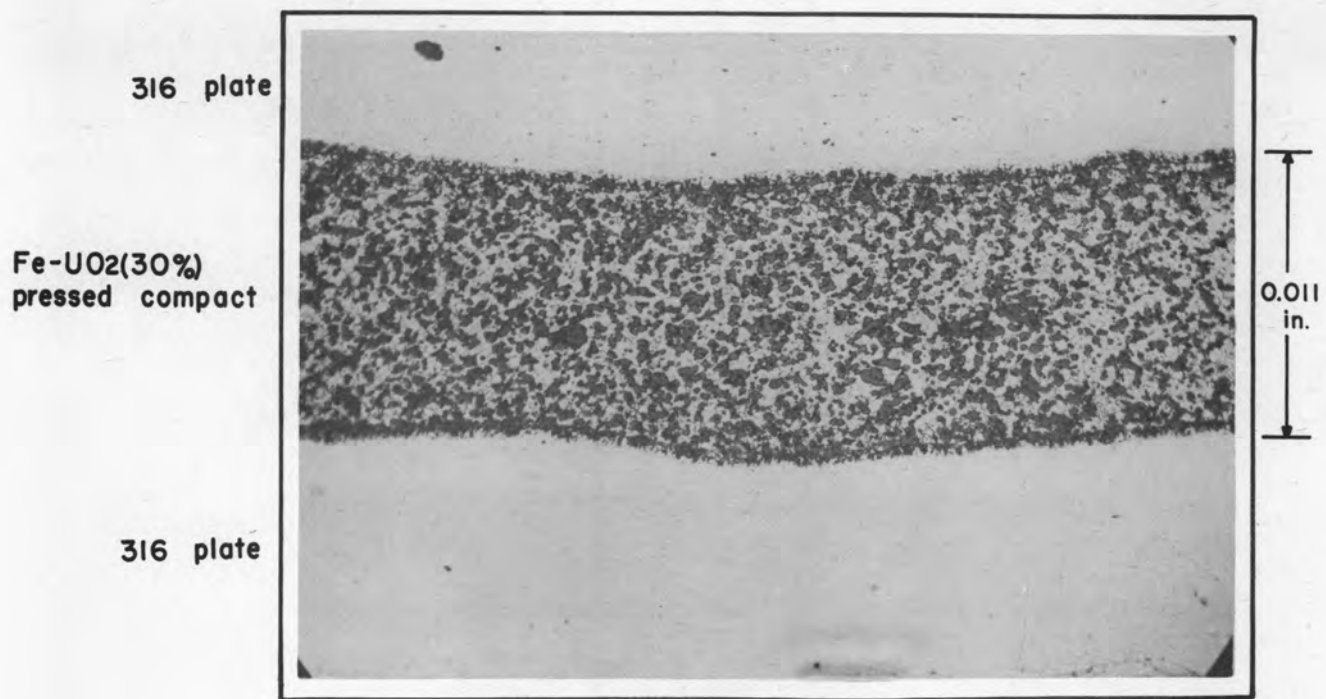


FIG. 3.13
175x

Y-3140

Double clad Fe-UO₂(30%) pressed compact. Hot rolled 88%.

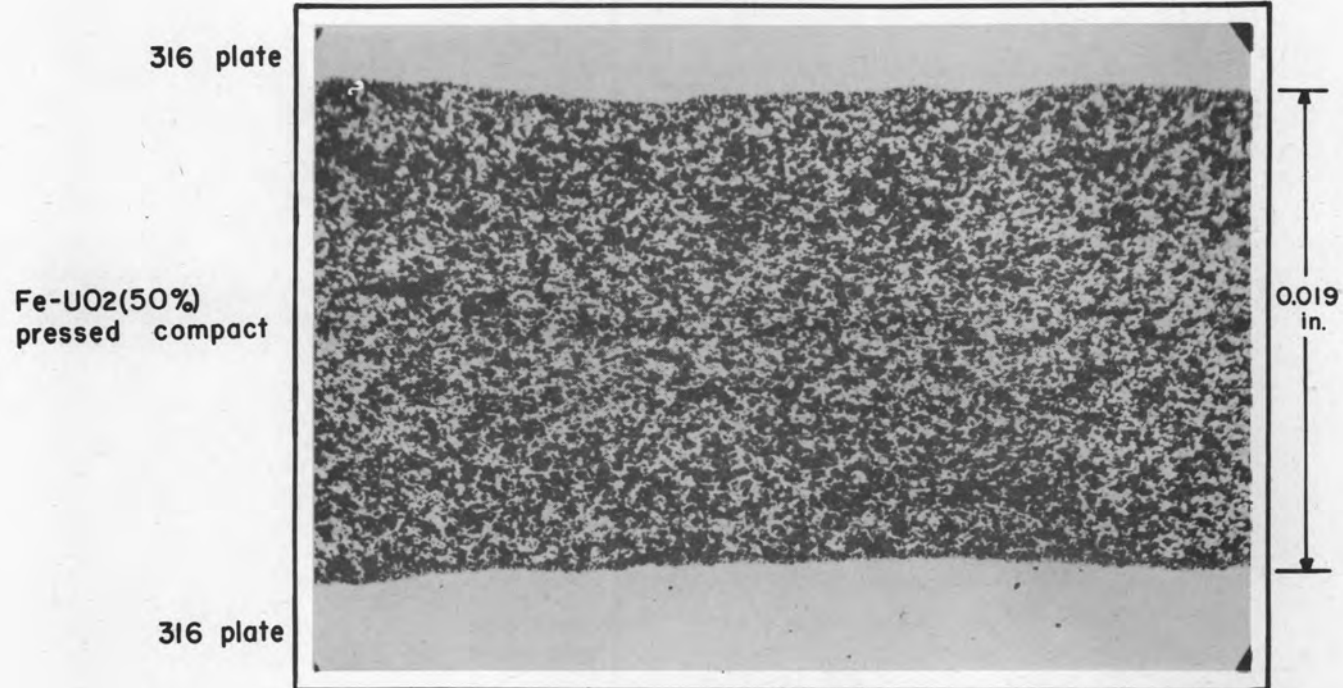


FIG. 3.14
175x

Y-3143

Double clad Fe-UO₂(50%) pressed compact. Hot rolled 78%.

The fabrication of fuel element sheets comprising substantial proportions of ceramic fuel (UO_2) supported and/or bonded by a metal matrix to metal face sheets is also being attempted utilizing a screen matrix.

Finely perforated or electroformed screen material has been obtained from commercial suppliers. Several preliminary diffusion or solid-phase bonding experiments were performed in which nickel screening was joined to both type 302 stainless steel and molybdenum face sheets. Results were not conclusive because of limitations of size of the available furnace; however, solid-phase bonding was evident for all materials used at approximately 1300°C for 1 hr, with a pressure of about 2 psi. Facilities are being assembled to accommodate larger specimens, higher unit loads, and accurate control.

The screens so far examined have been of two types. Electroformed screening is available in nickel, nickel with an overplate of chromium, copper, and copper with an overplate of nickel. A macrophotograph at $30\times$ of the C. Q. Jelliff Manufacturing Corp.'s 25- by 25-mesh Cu + Ni screen is presented in Fig. 3.15A. Figure 3.15B is a cross-sectional view at $180\times$ and shows concentric layers of electrodeposited nickel built up on a copper base grid. Figure 3.15C shows the 40 by 40 mesh grade in pure nickel.

Electroformed nickel or nickel + chromium screening available through the Pyramid Screen Company is shown at $30\times$ in Figs. 3.15D and E.

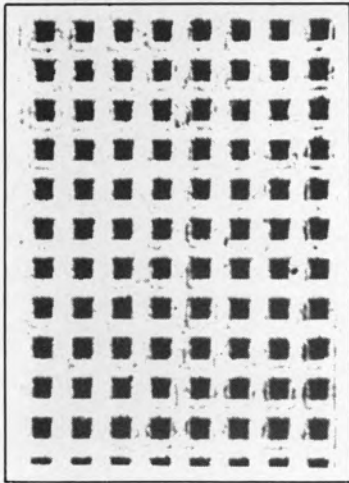
A contract is currently being negotiated with the Gerity-Michigan Corporation relative to development of various electroforming applications of interest.

Samples of mechanically perforated screening were supplied by the Hendricks Manufacturing Company. 25- by 25-mesh 0.020-in. diameter holes have been successfully punched in rolled molybdenum sheet 0.010 in. thick. The holes are clean and more sharply edged in contradistinction to those formed by electroforming processes. Figure 3.15F shows the upper surface of similar 25-mesh 0.010-in. steel sheet. Mechanical perforating is believed to be most feasible for fabrication of the screen type fuel matrix layer, since any desired metal or alloy sheet material is applicable. Limitations as to size of opening and particularly the percent total open area of such screening are currently being determined.

SCREENS

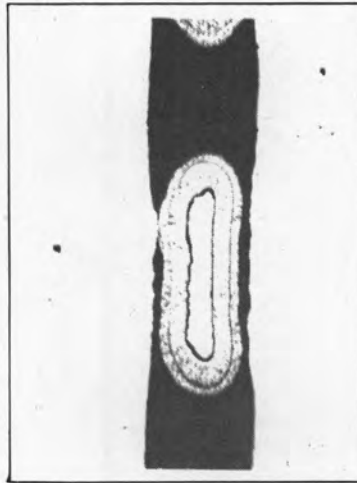
OFFICIAL USE ONLY
Y-3183

ELECTROFORMED AND PUNCHED



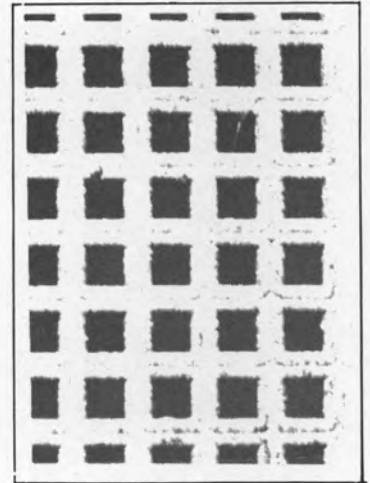
A
(30 X)

65 mesh/inch, 0.006" thick
Cu+Ni
ELECTRO



B
(180X)

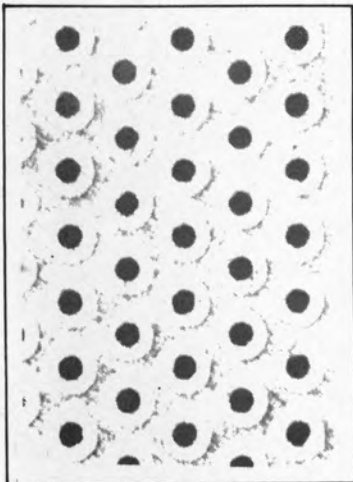
CROSS-SECTION OF
A - ETCHED



C
(30 X)

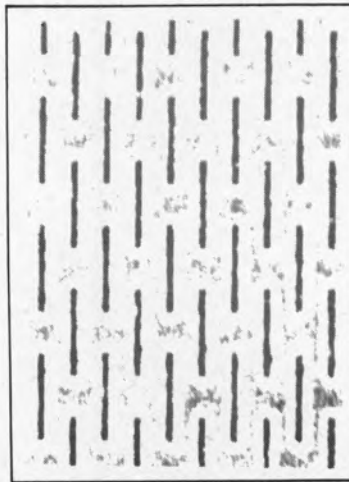
40 mesh/inch, 0.007" thick
NICKEL
ELECTRO

ALL MAGNIFICATIONS REDUCED
APPROXIMATELY 1/2 IN REPRODUCTION



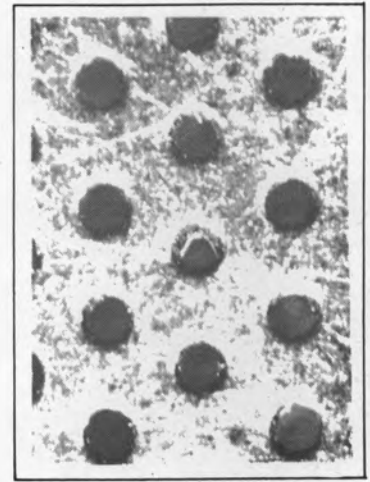
D
(30 X)

~45 mesh/inch, 0.0025" thick
NICKEL
ELECTRO



E
(30 X)

0.003" slot, 0.0035" thick
NICKEL
ELECTRO



F
(30 X)

25 mesh/inch, 0.010" thick
MILD STEEL
PUNCHED

FIGURE 3.15

Several experiments were performed to determine the practicality of loading of screen openings with UO_2 powder. By simply preparing a viscous slip of oxide and sodium silicate, a durable loading of intermediate density resulted. Relatively high-density UO_2 packings were achieved in preliminary tests by cold pressing UO_2 powder plus several percent paraffin binder into the screen openings. Steel dies with rubber and lead faced punches were employed, using pressures of 5 to 30 tsi compacting pressure. A radiograph of the loaded screens indicated that such procedures in general may be feasible.

Compatibility Test of Potential Fuel Element Materials. As a continuation of the program to investigate the mutual compatibility of possible fuel element components, further tests have been made.

The test procedure is essentially the same as that reported in ORNL-920 with the exception that a reduction of no more than 20% in diameter was attempted for the majority of tests. This was done since in earlier tests greater reductions quite often resulted in breaking the welds holding the end plugs, allowing the atmosphere of the furnace to reach the capsule contents. The time at test temperature was 100 ± 5 hr.

It should be emphasized again, as stated in ORNL-920, that these tests were set up to obtain qualitative information. The results, therefore, should be used with this inherent limitation in mind.

Whether or not a reaction had taken place was determined only by metallographic examination. No attempt was made to identify either the reaction products or their properties. Therefore the presence of a new phase would not in itself eliminate a given pair of materials since the new component may or may not cause decreased resistance to corrosion, radiation, or other types of damage.

It is felt, however, that, if intermetallics or alloys were formed, they would add to the already complex problem of matching thermal coefficients of expansion and maintaining reasonably continuous metallurgical bonds for maximum heat transfer. It follows that the presence of a reaction layer should serve as a warning that further investigation should be made before using a given pair of metals together.

In the tabulation of results (Table 3.7) the total thickness of all reaction layers is recorded along with any residual gap left between the components in the capsule. Although the origin of the gap could be due to a

TABLE 3.7

Compatibility Test Data

MATERIALS	TEMP. (°C)	REACTION LAYER (in.)	GAP (in.)	REACTION LAYER + GAP (in.)
Be vs. 316 SS	As-swaged at 1000	0.004	0.001	0.005
	1000	0.029	0.025	0.054
	900	0.006	0.014	0.020
	800	0.008	0.003	0.011
Be vs. 430 SS	900	0.004	0.008	0.012
	800	0.014	0.010	0.024
Be vs. Ni	1000	0.012	0.030	0.042
	800	0.025	0.002	0.027
Be vs. Inconel	1000	0.048	0.001	0.049
	800	0.019	0.019	0.038
Be vs. Mo	800	0.001	0.001	0.002
Be vs. Ti	1000	0.001	0.023	0.024
Be vs. Cb	1000	0.008		0.008
Be vs. Armco Fe	1000	0.005	0.010	0.015
	800		0.015	0.015
Be vs. Ta	1000	0.005	0.003	0.008
Be vs. UO ₂	1000	0.010		
Nb vs. UO ₂	1100	0.003		
Nb vs. BeO	1100	Slight reaction of undetermined depth since Cb rod dropped out; does not appear serious		
Mo vs. UO ₂	1100	No reaction		
Mo vs. BeO	1100	No reaction		
Mo vs. 316 SS	1100	0.001	0.001	0.002
Mo vs. 309 SS	1100	0.001	0.002	0.003
316 vs. UO ₂		0.002	This may be oxide due to poor evacuation; being checked	
316 vs. BeO	1100	No reaction apparent; to be rechecked		
316 vs. Cb	1100	0.001	0.001	0.002
316 vs. Ni	900	0.004		0.004
Inconel vs. Armco Fe	1100	0.004		0.004
	1000	0.002	0.002	0.004
	900	0.003		0.003
Inconel vs. 302	1100	0.001		0.001
	900	Trace reaction		

combination of effects such as (1) loss of reaction products during cutting for metallographic sample, (2) differences in thermal coefficients of expansion, and (3) change in the volume of the system through formation of intermetallic phases, it is felt that the presence of a gap is significant and would be undesirable in a fuel element.

CREEP-RUPTURE LABORATORY

If delivery schedules are met by the various vendors, installation of the laboratory equipment should be completed by the middle of February. Completion of the 14 special furnaces and the chamber for testing in vacuum or in inert atmosphere is expected in 30 to 60 days. These furnaces have been built partly by ORNL and partly by L. H. Marshall Co. The first unit has been delivered and the production schedule calls for two or three furnaces per week. Studies are underway on the first furnace unit to study the various operating characteristics, including the natural temperature gradient and the values and distribution of shunts to give an adequately long constant-temperature zone.

A 25-kw gasoline-driven motor generator with automatic transfer switch has been purchased to furnish emergency electrical power for the laboratory. Alternate sources for other services are provided but require manual switch-over. Man-power requirements have been surveyed and it is planned to have an operator in constant attendance.

A procurement program has been instituted to obtain sheet, rod, and tubing of the various materials that may be of interest to the ANP Project. Also requests have been placed with AEC to obtain alpha rolled uranium bar, and alpha and gamma extruded uranium bar for the Creep of Uranium Program. The production of test specimens of the several types and from the various materials has been discussed with the Research Shops. Tooling is being planned to provide specimens in lots of about 25 at a minimum production cost.

Owing to the lack of space in Building 2000 and the fire hazard involved in handling liquid metals, space has been obtained in the basement of the Pilot Plant Building to install a laboratory for stress-rupture testing in liquid-metal environments. This laboratory is in the preliminary design stage. It is planned to install four tube burst units and six lever arm type

creep racks along with the necessary instrumentation and other auxiliaries. The planning includes possible future expansion if the program at that time indicates such an expansion to be desirable. The furnaces and test chambers to contain the specimens and liquid metal are in the final design stage. Considerable attention has been given to the design problems in order to minimize the handling of the liquid metal and the hazards. This laboratory will also be under the 24-hr supervision of an operator.

No tests have been conducted during the past quarter in the Creep Laboratory. During this construction period the room has been crowded with the service crews and the power has been frequently interrupted, making testing impractical.

Eighteen tensile tests were conducted at 1500°F to observe the deformation and recovery characteristics of types 310, 316, and 347 stainless steel and Inconel under conditions of cyclic stressing. The tests were conducted at two constant strain rates, 0.05 and 0.10 in./min. The strain rate was maintained constant during loading until the load ceased to increase, then the load was released slowly. The specimen was held at zero stress for 10 min prior to reloading. This procedure was repeated for four or five cycles, giving a total test time of approximately 1 hr.

The series has just been completed, and the data have not yet been adequately studied. Detailed data will be reported at a later date. Following are a few generalized observations:

1. Increasing the strain rate markedly increased the maximum stress obtained.
2. Generally, the maximum stress obtained in each cycle decreased with each successive stress cycle.
3. Under the test conditions elastic recovery was not detected.

WELDING LABORATORY

Housing construction for the Welding Laboratory has recently been completed. It is expected that most of the heliarc welding equipment and associated apparatus will be delivered and in operation during February. A

research program for the production of welded test specimens using materials of interest to the ANP Group will be underway during February. This study will be conducted using the facilities of the Welding Laboratory and the services of a skilled welder recently assigned to the Metallurgy Division.

Welding of Refractory Metals. Experiments in welding of molybdenum have been delayed pending the completion of facilities of the Metallurgy Division Welding Laboratory. A research contract has been awarded the Battelle Memorial Institute to investigate the weldability of high-purity molybdenum.

Thermal Convection Loop Fabrication. At the request of the Dynamic Corrosion Group supervision of the fabrication of harps was undertaken by the Welding Section. Joint design and welding sequence was specified for a series of eight harps, which were constructed in the Research Shops. The harps have been leak tested and turned over to the Experimental Engineering Group for testing in liquid metal.

A group of eight 400-series stainless steel harps is being prepared for fabrication. Since this group of loops is of a new design, joint design and welding sequence specifications will be prepared.

Seam-welding of Flattened Tube Ends. At the request of the Static Corrosion Group a study is being undertaken to determine the feasibility of using resistance seam-welding to seal off the flattened ends of tubes containing solidified metal under consideration as a liquid coolant. Preliminary results indicate that vacuum-tight seals can be obtained by using the following technique:

1. Flattened tube ends were inserted in a slot between two sheets whose total thickness equalled the thickness of the flattened tube end.
2. A resistance seam weld was initiated on the sheet material and continued across the tube end onto the remaining sheet material and was internally flushed with argon during welding.
3. The tube was removed and vacuum tested.
4. After being filled with liquid metal, the other tube end was flattened and seam-welded as above while under evacuation, using a mechanical pump.

Elevated temperature tests are underway for further evaluation of this technique.

PHYSICAL CHEMISTRY OF LIQUID METALS

Hydrogenous Fluids. A study is to be undertaken to determine the approximate liquidus curves for systems containing a high percentage of hydrogenous compounds. The purpose of this study is to determine what systems might be useful as moderator-coolants in a high-temperature reactor on the basis of melting point. Subsequent studies are planned to determine the stability of selected mixtures and to establish methods of decreasing undesirable dissociation. The necessary apparatus for conducting the liquidus curve determinations is being designed.

Corrosion of Metal Single Crystals by Liquid Metals. A fundamental study is being undertaken of the corrosion of large metal single crystals by liquid metals. The apparatus to be used in the initial phase of this study has almost been completed.

Large single crystals should be the most satisfactory specimens for this fundamental study. An ordinary polycrystalline metal surface is an exceedingly complex system. Even if the complicating factors of mechanical strain, foreign films, and roughness are removed, a polycrystalline metal surface still consists of a large variety of crystal faces and boundaries. Studies of the physical chemistry of a great many surface phenomena have shown that the velocity of nearly every rate process differs markedly on different crystal faces.⁽¹⁾ Frequently these differences prove to be of several orders of magnitude, as in the case of the oxidation of copper at intermediate temperatures.⁽²⁾ In other instances it has been found that entirely different processes take place on different crystal faces, as in the case of the catalytic decomposition of CO on Ni.⁽³⁾ The physicochemical properties of an ordinary metal surface are a composite of the separate properties of the various crystal faces exposed. In order to understand the behavior of a metal surface it is necessary to understand the properties of the different crystal faces.

A study of the action of liquid metals on the various faces of metal single crystals is being undertaken in order to determine what influence

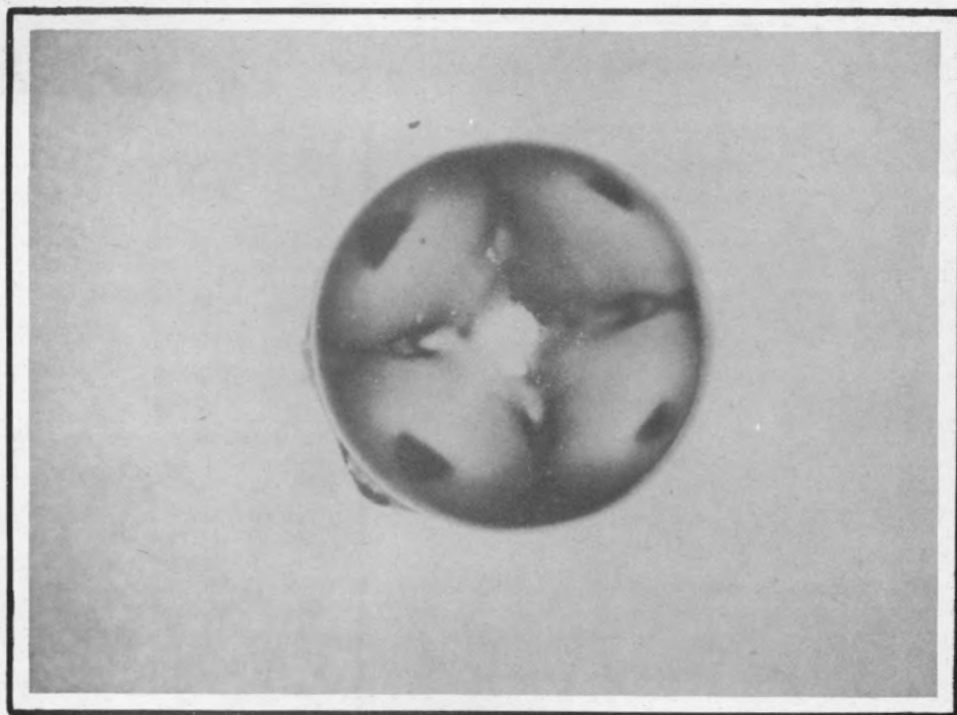
- (1) Tamman, v. G., and Sartorius, F., "Atzerscheinungen am Kupfereinkristall," *Z. anorg. allgem. Chem.* 175, 97 (1928); Gwathmey, A. T., Leidheiser, H., Jr., and Smith, G. P., "Influence of Crystal Plane and Surrounding Atmosphere on Chemical Activities of Single Crystals of Metals," *National Advisory Committee for Aeronautics*, Tech. Note No. 1460 (1948).
- (2) Gwathmey, A. T., and Benton, A. F., "The Reaction of Gases on the Surface of a Single Crystal of Copper. I. Oxygen," *J. Phys. Chem.* 46, 969 (1942).
- (3) Leidheiser, H., Jr., and Gwathmey, A. T., "The Selective Deposition of Carbon on the (111) Face of a Nickel Crystal in the Catalytic Decomposition of Carbon Monoxide," *Am. Chem. Soc. J.* 70, 1206 (1948).

crystal orientation may have on liquid-metal corrosion. Very little information exists on this subject. Therefore, initial studies will consist of a qualitative survey of representative liquid metal--single crystal systems to determine if the expected differences occur, and to determine what crystal faces are most active in a given process. On the basis of this qualitative information it should be possible to select favorable conditions for quantitative studies of such phenomena as may be encountered.

The solid-metal specimens used in this survey will consist of spherical single crystals up to 5/8 in. in diameter. Spherical specimens offer a unique advantage in making qualitative studies. Every possible crystal face must occur at least twice on the surface of the sphere. Therefore all crystal faces may be simultaneously compared in a single experiment. An example of the type of result obtained is given in Figs. 3.16 and 3.17.

The photographs show a single crystal sphere of copper, the surface of which was initially electrolytically polished until very smooth and then etched electrolytically in an orthophosphoric acid solution. The pattern resulting from different rates of etching attack on different crystal faces may be seen in Figs. 3.16 and 3.17. In Fig. 3.16 a [100] axis is normal to the plane of the page. Copper has a cubic crystal lattice and the expected fourfold symmetry of the (100) pole may be seen. The (100) pole itself is the geometrical center of the fourfold symmetry. In Fig. 3.17 a [111] axis is normal to the plane of the page. The expected threefold symmetry may be seen. All the other crystallographic poles may be located in like manner, using the methods of crystallography. For example, a (110) pole lies midway between any pair of adjacent (100) poles or any pair of adjacent (111) poles.

Where practical, the experimental procedure will be as follows: The spherical single crystals will be electrolytically polished until the cold-worked surface layers have been substantially removed, as indicated by the sharpness of electrolytic etch patterns and until a very smooth surface is obtained. Then the crystals will be annealed, preferably in an atmosphere in which their oxide films are reduced. Finally, the crystals will be immersed in the liquid metal without exposure to the atmosphere. An apparatus for conducting such studies with liquid metals which do not attack quartz is almost completed. The first experiments with this apparatus will be made on the mercury-copper system because of the ease of handling mercury and the immediate

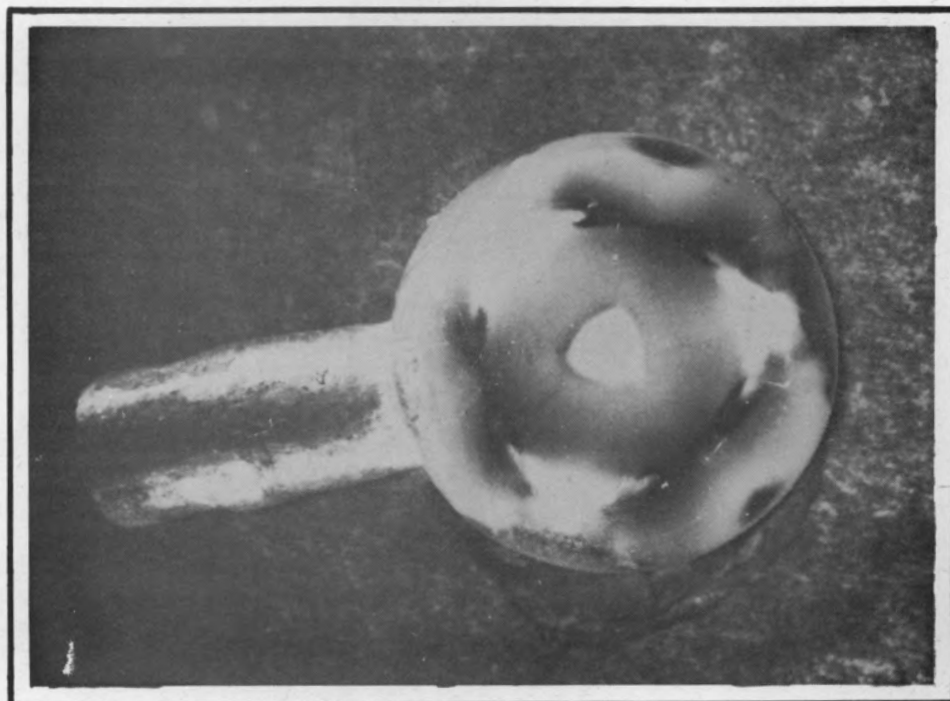


Y-3122

A

4X

FIG. 3.16 ELECTROLYTIC ETCH PATTERN ON $5/8$ INCH DIAMETER COPPER SINGLE CRYSTAL. PHOTOGRAPH NORMAL TO (100) AXIS. (FOURFOLD SYMMETRY)



Y-3123

B

4X

FIG. 3.17 ELECTROLYTIC ETCH PATTERN ON $5/8$ INCH DIAMETER COPPER SINGLE CRYSTAL. PHOTOGRAPH NORMAL TO (111) AXIS. (THREEFOLD SYMMETRY)

availability of spherical single crystals of copper.

A single inelegant experiment has been performed. It was found that certain sharply defined crystallographic regions of a spherical copper crystal were wetted by mercury to give a uniform film while all other regions were covered with fine droplets. This result is of a preliminary nature.

Obtaining suitable spherical single crystals presents some problems. A great many metal crystals may be grown by the Bridgman method, and some of these are available commercially. Crystals which must be formed by other methods are difficult to obtain commercially. It may prove necessary to set up suitable facilities at ORNL for the growth of crystals by the Andrade and halide decomposition methods.

The machining of spherical single crystals so as to produce a cold-worked layer which can be substantially removed by electrolytic polishing is a research problem. For some metals this can be done with reasonable success but for others it may prove necessary to grow the crystals in a spherical shape. The most frequent trouble in machining single crystals is encountered with crystals which may be fractured by cleavage. In such cases it is sometimes observed that abnormal corrosion occurs along cleavage planes in such a manner that deep cracks are formed even though such cracks were not observed before corrosion.

Physicochemical processes occurring at a surface are frequently sensitive to the method by which the surface was prepared. Although this is generally recognized, it has received little experimental attention. It may prove desirable to conduct studies on surface preparation. However, during the period in which the major emphasis is on a qualitative survey of corrosion, such secondary research as surface preparation will be avoided except where it is necessary to make the corrosion results meaningful.

4. MTR FUEL ELEMENTS

During this period 20 additional modified MTR fuel elements were manufactured for use in the Bulk Shielding Reactor, thus completing the order. Orders have been placed for auxiliary components for the 138 MTR fuel assemblies as follows: (1) end boxes, (2) combs, (3) retaining and beveled rings, (4) retaining springs, (5) aluminum plates, and (6) side plates.

The new 31-ton mechanical press for punching cores and frames has been installed. Dies are in the shop, 35% complete. One shim-safety fuel section was made to test a new design of this part of the MTR. Editing of the report covering MTR mock-up fuel rod production was completed. It will be issued as ORNL-951.

A request was made for additional man power and equipment for full-scale MTR fuel rod production (2.3 rods per day). These will be needed after completion of the original order of 138 assemblies, about October 1, 1951.

5. SERVICE WORK

The bulk of the effort of the last quarter that can be classified as service work was on the following:

1. Production of enriched U-Al alloy disks for the KAPL critical experiment.
2. Rolling large ingots of Boral for Brookhaven and the MTR.
3. Production of enriched uranium metal disks for the ANP critical experiment.

The first two were completed, and the last is about one-third completed.

KAPL DISKS

Production of about 20,000 enriched U-Al alloy disks for the KAPL critical experiment was completed in November 1950. X-ray diffraction patterns of the gray powder found in blisters of defective disks were unidentifiable. This blistering can probably be traced to hydration of segregated aluminum oxide in the ingot.

BORAL ROLLING

Fifty-four ingots of Boral were cast and jacketed at Y-12 and subsequently rolled at X-10 on the 20- by 30-in. Mesta mill. Initially the ingots were 26 by 28 by 1½ in. and weighed about 75 lb. Since only one furnace that could handle this size was available, production was severely limited, and the size was later cut to 20 by 26 by 1½ in. so that another furnace could be utilized. Ingots were preheated a minimum of 2 hr at 1100°F and rolled without reheating. Four were rolled to 1/8 in. and 50 to 1/4 in. Total rolling time per ingot was 3 min.

ANP DISKS

At the request of A. D. Callihan, 6000 disks of enriched uranium metal are being fabricated for a criticality experiment to be run in connection with the ANP Program. Original specifications were as follows:

QUANTITY	DIAMETER (in.)	THICKNESS (in.)	MASS (g)
3000	2.860 + 0.000 - 0.004	0.010 ± 0.0005	19.5 ± 0.5
3000	1.430 + 0.000 - 0.002	0.010 ± 0.0005	4.87 ± 0.13

Each disk was to have a 0.196-in. hole centered within 0.001 in.

Ingots weighing about 1 kg each and with dimensions about 1/8 by 4 by 7 in. are being supplied by Y-12. These are cold rolled to 0.050 in., a total reduction of 60% without cracking. This high ductility is somewhat remarkable and is indicative of the high purity of the material. The rolling equipment presently installed at X-10 is not well suited to precision rolling of thin foils because of the large roll diameters. To reduce the metal to 0.010 in. it is necessary to resort to pack rolling. The 0.050-in. stock is encased between plates of 1/8-in. steel, the edges are welded, and the sandwich is hot rolled at 1200°F. The jackets are then removed and disks are punched.

Initially, grossly overweight disks were pickled with dilute HNO₃ to attain the desired weight. Small weight adjustments were then made by punching small holes in the disks. It was found that the oxide layer on disks which had not been etched presented a serious contamination problem. Consequently it was decided to pickle all disks. The etching procedure now in use is as follows:

1. Dip in cold concentrated HNO₃.
2. Rinse in three water baths.
3. Dip in acetone.
4. Dry.

The weight tolerances were then adjusted downward to allow for the loss of uranium in the pickling baths as follows:

Small disks	4.42 to 4.52 g
Large disks	17.70 to 18.10 g

To date, 1500 (about 30 kg) of the large washers have been finished.

~~SECRET~~

METALLURGY DIVISION PERSONNEL*

As of January 31, 1951

Abrams, L. A.	Drostén, F. W.	Ogle, J. C.
Adams, R. E.	Easton, D. S.	Oliver, R. B.
Adamson, G. M.	Erwin, J. H.	Patriarca, P.
Andersen, A. G. H.	Fitzgerald, R. L.	Poe, D. V.
Atchley, N. M.	Flynn, J. B.	Pope, J. E.
Banker, L. E.	Frye, J. H., Jr.	Proaps, W. W.
Beaver, R. J.	Fulton, T. W.	Rosson, D. E.
Betterton, J. O., Jr.	Glasgow, L. G.	Shubert, C. E.
Bomar, E. S., Jr.	Goldston, G. D.	Smith, C. D.
Borie, B. S., Jr.	Gonzalez, G. M.	Smith, C. L.
Boss, G. H.	Gower, J. C.	Smith, G. P., Jr.
Boyd, E. R.	Gray, R. J.	Steele, R. M.
Boyle, E. J.	Griggs, E. P.	Thomas, M. J.
Brasunas, A. D.	Hamby, D. E.	Trotter, L. R.
Bridges, W. H.	Hix, J. N.	Turner, J. P.
Buker, D. O.	Hudson, R. J.	Wallace, H. J.
Byrum, B. F.	Jacox, D. J.	Wallace, R. M.
Carr, H. T.	Jetter, L. K.	Weaver, C. W.
Cooley, G. E.	Johnson, R. W.	Webb, R. S.
Crouse, R. S.	Layne, E. E.	White, J. R.
Cutcher, C. F.	Leslie, B. C.	Williams, R. O.
Cunningham, J. E.	Manly, W. D.	Woods, J. C.
Day, R. B.	Miller, E. C.	

*The Physics of Solids Institute now issues its own quarterly report. Its personnel consists of 27 scientists, three technicians, and one clerical worker, a total of 31.

~~SECRET~~